國　立　交　通　大　學
光　電　工　程　學　系　碩　士　班

碩 士 論 文

利用新穎材料提升氮化鎵太陽能電池的效率

Enhanced Power Conversion Efficiency of GaN-Based Solar Cell by Novel Materials

研究生：曹庭耀

指導教授：郭浩中教授

謝嘉民教授

中 華 民 國 一 百 零 一 年 七 月

利用新穎材料提升氮化鎵太陽能電池的效率

Enhanced Power Conversion Efficiency of GaN-Based Solar Cell by Novel Materials

研究生：曹庭耀　　Student：Ting-Yao Tsao

指導教授：郭浩中 教授　　Advisor：Hao-Chung Kuo

謝嘉民 教授　　Jia-Min Shieh

國立交通大學

光電工程學系碩士班

碩士論文

A Thesis

Submitted to Photonics Institute

College of Electrical Engineering

National Chiao Tung University

in Partial Fulfillment of the Requirements

for the Degree of

Master

In

Photonics

July 2012

Hsinchu, Taiwan, Republic of China

中華民國一百零一年七月

利用新穎材料提升氮化鎵太陽能電池的效率

研究生：曹庭耀　　指導教授：郭浩中 教授

謝嘉民 教授

國立交通大學光電工程學系碩士班

摘要

在本論文中，我們針對氮化鎵太陽能電池的反射率高於 20%而導致效率不佳的問題來做一個改良，另一部份是針對氮化鎵太陽能電池短波段的入射光被表面的透明導電層所吸收而導致短波段光都浪費掉的問題來做一個改善，主要是針對這兩個問題而改進進而提升我們氮化鎵太陽能電池的效率。

本論文第一部分是在討論如何改善反射率高的問題，很多文獻顯示，我們如果在表面製作奈米結構可以達到降低反射率的效果。所以我們製作具有奈米結構的 PDMS 模，這種模製程可以大面積而且便宜方便，不需要像其他做奈米結構要在真空下面進行，而且我們發現這樣製作出來的 PDMS 模具有很好的抗反射的效果，而且不只這樣，這種模也具有讓光散射的效果，讓光在電池裡行徑路徑比較長，有利增加我們效率。之後，我們將此種具有降低反射效果的 PDMS 模應用在我們氮化鎵太陽能電池上，並針對元件之反射率、外部量子效應、光電轉換效率等來進行分析，並以變角度反射率量測來證明次波長結構在變角度下仍然有不錯的抗反射效果，因此我們觀察到全波段量子效率的提升，將此具有 PDMS 模的電池相較於沒有 PDMS 模的電池，提高了 7.2%光電流增加與光電轉換效率 7.1%的增強，有效驗證了 PDMS 模對於氮化鎵太陽能電池光電轉換效率之提昇是有幫助的。

本論文第二部分是在針對氮化鎵太陽能電池短波段的入射光被表面的透明導電層

所吸收而導致短波段光都浪費掉的問題來做一個改善。因為短波長紫外光區域具有全太陽頻譜 7%，如果我們可以好好利用這些光會對我們效率有很大的幫助。

所以我用了量子點(quantum dot)，我們選用 400nm 的 CdS 量子點，這種量子點會吸收在 400 以前的光進而再放射出 400nm 左右的可見光，可以被我們氮化鎵太陽能電池所吸收利用，我們是在做好的元件上面點上我們的量子點讓它在表面是一層膜，他就可以在 ITO 吸收短波長之前吸收我們的短波長的光，而放射出 ITO 吸不到的波段給我們電池使用，這樣就不會有之前提到的浪費的能量。之後我們將有點量子點的電池相較於沒有量子點的，提高了 6.3%光電流增加與光電轉換效率 7.2%的增強，有效驗證了量子點對於氮化鎵太陽能電池光電轉換效率之提昇是有幫助的。

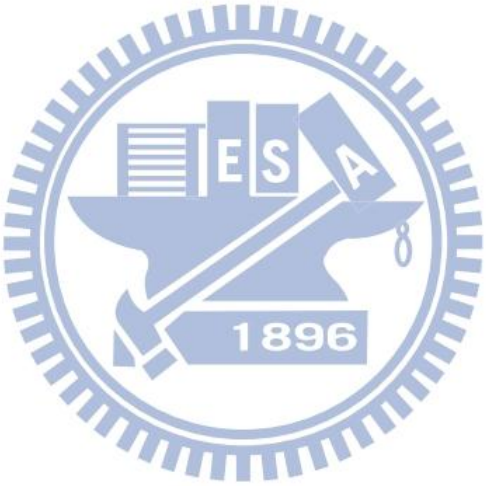

Enhanced Power Conversion Efficiency of GaN-Based Solar Cell by Novel Materials

Student：Ting-Yao Tsao　　Advisors：Hao-Chung Kuo

Jia-Min Shieh

Photonics Institute

National Chiao Tung University

Abstract

The InGaN/GaN multiple quantum well solar cell was considered for future generation of photovoltaic applications due to the high efficiency. However, due to the high reflectance, and the high absorption by ITO at short wavelength region. The efficiency is limited. How to improve light harvesting is a very important issue in high efficiency InGaN/GaN multiple quantum well solar cell. Antireflection and photo collection are key techniques for efficiently harvesting solar photon.

For the first problem, Several studies of nanostructure offer ultra-low reflectivity, another feature of nanostructure is diffraction of light, which get longer optical path length and then further enhance the light absorption. Here we use textured PDMS film to solve the problem. The advantages of using PDMS film are the low-cost, non-vacuum system and simple process (only spin coating and imprinting needed). PDMS film provides a refractive index gradient to serve as an anti-reflection layer. Extra benefits of light trapping and scattering can be added when the film is stamped with high texture pattern.

We demonstrated the textured PDMS film is useful in harvesting solar photon and enhancing the power conversion efficiency of InGaN/GaN multiple quantum well solar cell. Compared with a flat InGaN/GaN multiple quantum well solar cell, the power conversion efficiency achieved 7.1% enhancement, and the J_{sc} achieved 7.2% enhancement respectively.

Second part we will solve problem for the high absorption by ITO at short wavelength region. So the UV region light loss in the process. We use quantum dot(QD) to solve the problem. This CdS QD layer is capable of converting ultraviolet photons (λ<400nm) to the visible blue band. So we can spread the quantum dots on the cells, it can absorb the UV region light before ITO layer and converting to visible region light that ITO can not absorb. In this way, we can solve the problem mentioned before, just by adding some CdS quantum dots material.

We demonstrated the quantum dots is serve as the down conversion center of the light in InGaN/GaN multiple quantum well solar cell. Compared with a InGaN/GaN multiple quantum well solar cell without quantum dots, the power conversion efficiency achieved 7.2% enhancement, and the J_{sc} achieved 6.3% enhancement respectively.

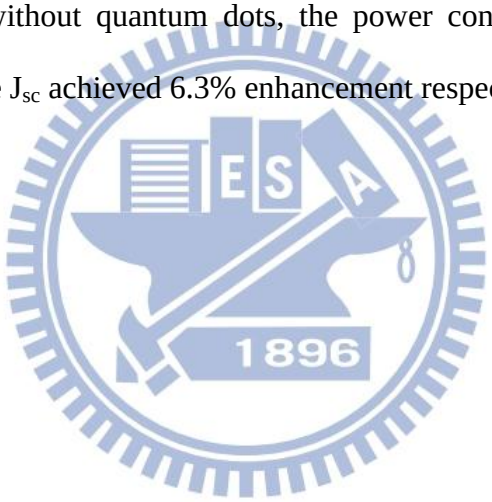

Acknowledgements

兩年的碩士班生涯一下子就走到終點了，現在還依稀記得第一次踏進實驗室的感覺，當初會選擇這間實驗室是因為感覺實驗室氣氛融洽，而且可以學習到很多知識，現在也驗證當初的選擇是對的。首先，我要感謝郭浩中教授和謝嘉民教授，老師的耐心指導以及提供寶貴的意見，讓我在碩士班這個階段學習到很多做研究和分析實驗的結果。這些教授們提供的無價之寶我相信在未來的道路上依舊受用無窮，也謝謝郭老師提供我很好的研究環境，還有平實的鼓勵與勉勵，讓我在這兩年能夠順順利利在研究上面有成果。也謝謝賴芳儀老師對我的指導和勉勵。

感謝當初把我拉進實驗室的閔安學長，我在學長身上學習到很多東西。還要感謝信助學長，幫助我很多，也謝謝平時的鼓勵與勉勵。還要特別謝謝 90 學長，90 對待我們就像朋友一樣，我在 90 身上學長很多專業和處理事情的態度，真的很敬佩學長，我很幸運是給 90 學長帶到，也謝謝 90 平時的鼓勵和勉勵。另外我還有感謝肉哥、祐廣、珣彣、BoBo、蛋黃、國儒、Joseph、李博、David、小見、柏孝等學長對我的指導和照顧。再來，我也要感謝懷祥施、鈞凱學弟和芸林學妹，感謝你們全力協助讓我可以順利畢業，希望學弟妹也可以順順利利的準時畢業，真的很感謝你們。

此外，我要感謝讓我在這兩年的研究生涯充滿樂趣的實驗室夥伴們，我永遠都會記得我們碩一喝酒團，每天做完實驗晚上喝酒的日子，謝謝老瀚、魔王、小蔡、盛雲和阿賢。有了你們碩班生涯一點都不無聊，很感謝能讓我在交大這個宅宅的環境遇到同好，我真的太幸運了。相信我們友誼會一直存在，之後就一起賺大錢然後再出來喝掛吧，再來看小蔡把酒倒掉的樣子。也謝謝雨婷、Bush、炫庭、球男、萬海、家銘、國軒、宇志，因為有你們使我碩班增添很多美好的回憶，以後有時間大家一定要再出來聚聚。

最後我要感謝我阿婆還有我爸媽、媽咪、弟弟妹妹們，因為有你們的支持我才可以再撐過這兩年，謝謝你們總在我心情不好給我鼓勵。感謝臭米摸一直陪在我身邊，陪我度過最艱難的時光，在你身邊很幸福，我愛你。

這本論文能夠產出真的很謝謝各位幫忙，沒有你們我不可能順順利利，希望大家在未來道路上能夠心想事成，期待再次相逢的日子。

Content

List of Tables

List of Figures

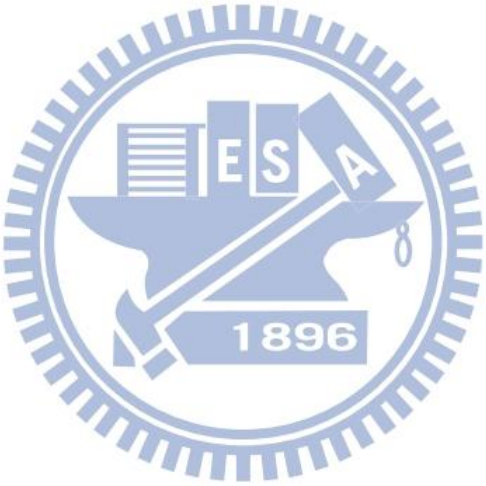

Chaper 1. Introduction

Since the development of the global environment has passed hundreds of thousands of years, as technology advances and the development of capacity and population growth, growing demand for expansion of the Earth's resources. IEA (International Energy Agency, IEA) mentioned in 2007 and 2030 global energy demand will grow by 1.5% at World Energy Outlook 2009, while after 2030 the world's electricity demand is expected to increase the rate of 2.5% per year [1]. Coal is still the main fuel of power generation industry. However, the one of main cause is derived from the carbon dioxide caused by continued growth in global carbon dioxide emission. This will certainly lead to a long large-scale climate change. It will give the irreparable harm to the earth. So, how to effectively reduce carbon dioxide emission is the common face of the issue.

In this regard, an energy revolution can be expected, and the rise of green energy will play a big lead of the energy revolution. The green energy is a reusable and less polluting energy sources, such as wind, solar, geothermal, tidal, hydropower, only solar cells is a one-step conversion process which directly convert sunlight into electricity. Solar energy is also a very environmental protection renewable energy, the process converting sunlight to electricity does not produce waste and exhaust emissions, so it will not produce any pollution to water, air, and soil. Solar energy has a very large number of sources of supply. Because the sun produces about 1.76 × 105 MW energy per year, of which 600 MW irradiation on the surface of the earth are available. Its energy is 100,000 times than the global average power. If we can use the solar energy effectively, we can not only solve the threat of energy depletion, but also solve the environmental problems caused by the greenhouse effect. Therefore solar energy will be the most important renewable energy source in the future. (Figure 1-1).

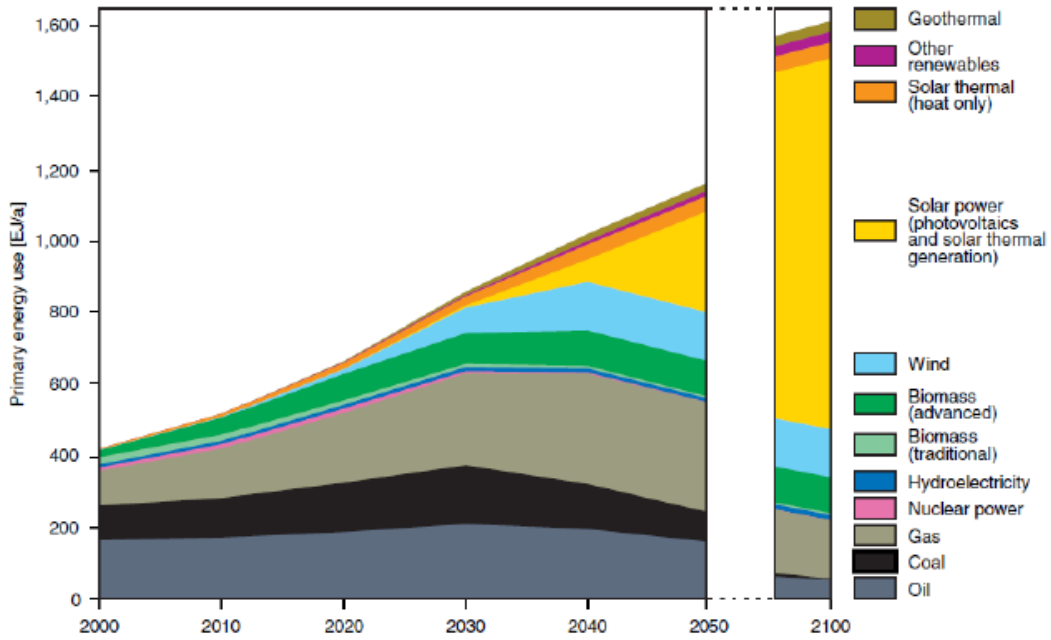

Figure 1-1 The amount of energy usage in next 100 years (German Advisory Council on Global Change WBGU Berlin 2003)

1.1 Brief development of the solar cell

The development of the solar cell stems from the work of the French physicist Antoine-César Becquerel in 1839. Becquerel discovered the photovoltaic effect while experimenting with a solid electrode in an electrolyte solution; he observed that voltage developed when light fell upon the electrode. About 50 years later, Charles Fritts constructed the first true solar cells using junctions formed by coating the semiconductor selenium with an ultrathin, nearly transparent layer of gold. Fritts's devices were very inefficient, transforming less than 1 percent of the absorbed light into electrical energy.

By 1927 another metal-semiconductor-junction solar cell, in this case made of copper and the semiconductor copper oxide, had been demonstrated. By the 1930s both the selenium cell and the copper oxide cell were being employed in light-sensitive devices, such as photometers, for use in photography. These early solar cells, however, still had

energy-conversion efficiencies of less than 1 percent. This impasse was finally overcome with the development of the silicon solar cell by Russell Ohl in 1941. In 1954, three other American researchers, G.L. Pearson, Daryl Chapin, and Calvin Fuller, demonstrated a silicon solar cell capable of a 6-percent energy-conversion efficiency when used in direct sunlight. By the late 1980s silicon cells, as well as those made of gallium arsenide, with efficiencies of more than 20 percent had been fabricated. In 1989 a concentrator solar cell, a type of device in which sunlight is concentrated onto the cell surface by means of lenses, achieved an efficiency of 37 percent due to the increased intensity of the collected energy.

Generally there are two major types of solar cell, the first one is organic solar cell and the second one is inorganic solar cell. Due to the short lifetime and low conversion efficiency, the development of organic solar cell was limited. There are many types of inorganic solar cells, the main solar cells materials are compound semiconductor materials which include Ⅱ - Ⅵ(CdS / CdTe) and Ⅲ - Ⅴ, silicon (crystalline, poly-crystalline, amorphous)[2-4]. Figure 1.1-1 shows the highest conversion efficiency of various solar cells. CdS / CdTe solar cell is not a wise choice due to cadmium inhalation or ingestion will accumulate in the human liver and cause kidney poisoning, therefore the manufacturing processes waste which will cause environmental issues. The advantage of Ⅲ - Ⅴ compound solar cells is ultrahigh power conversion efficiency, the power conversion efficiency of single-junction GaAs solar cell is about 18% [5] and the efficiency of the three junction of Ⅲ - Ⅴ solar cells can up to 30% [6], furthermore it has a good anti-radiation property so it is very suitable for the satellites or space application. However, the cost of Ⅲ - Ⅴ compound wafer is very high, such as GaAs , InP, etc., and it is a complex epitaxial technology, so it is not suitable for universal power applied to the people's livelihood. The way to reduce the cost of Ⅲ - Ⅴ solar cells is using concentrating system, which can greatly reduce the usage of Ⅲ - Ⅴ material furthermore to reduce the costs.

Silicon base material which include single crystalline silicon, polycrystalline silicon and amorphous silicon, because of the mature process technology of single crystalline silicon and poly crystalline silicon materials, so the earliest solar cell was the crystalline silicon solar cells and the power conversion efficiency of single crystalline silicon solar cell is around 20%, so the market share of crystalline silicon solar cells is nearly 90%. But the efficiency of silicon base solar cell is only16~17%. If we need about 1GW electrical power, we need about hundred million of 12 inch silicon high quality wafer to achieve. This make it impossible, so the high efficiency Ⅲ - Ⅴ solar cells will replace silicon base solar cell is a tendency in the future.

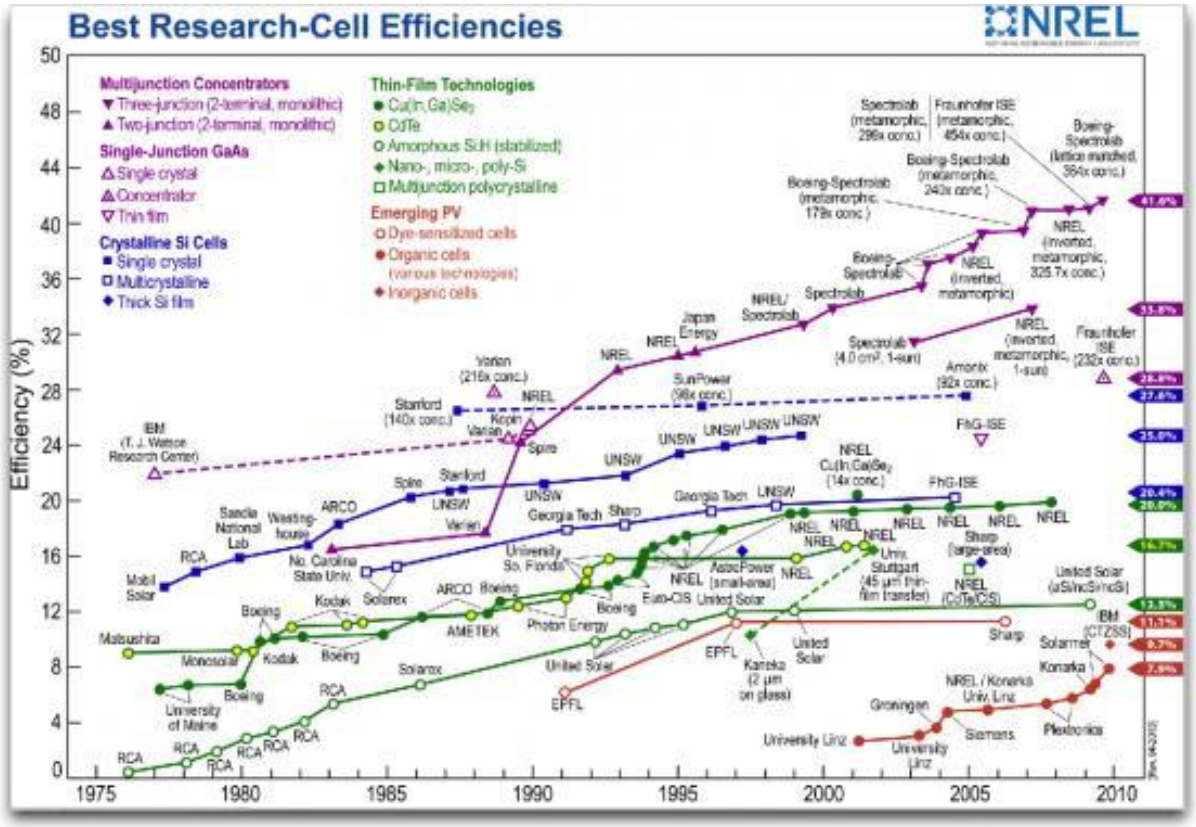

Figure 1.1-1 The highest conversion efficiency of various solar cells (Res. Appl.17, 85-94 2009)

1.2 Introduction of GaN-Based solar cells

III-nitrides are ideally suited to the fabrication of optoelectronics devices such as lasers and light-emitting diodes, due to their high efficiency and wide applicability. The properties of III-nitrides include large carrier mobility, high drift velocity, strong optical absorption, and resistance to radiation, making them ideal for the development of photovoltaics.

1.2.1 The characteristics of InGaN

GaN-based photovoltaics with an $In_xGa_{1-x}N$ absorption layer are promising these years. InGaN alloys have been widely exploited as active materials for light-emitting diodes and laser diodes with emission wavelengths covering from near UV to green spectral regions. InGaN alloys recently emerge as a new solar cell materials system due to their tunable energy band gaps (varying from 0.7 eV for InN to 3.4 eV for GaN), covering almost the whole solar spectrum and superior photovoltaic characteristics such as direct energy band gap in the entire alloy range and high carrier mobility, drift velocity, radiation resistance, and optical absorption of ~10^5 cm^{-1} near the band edge.

InGaN alloys have been shown to have superior high energy radiation resistance for space based PV applications. The band gap of InN was recently discovered to be 0.7 eV as opposed to the previously believed 1.3 eV. The importance of this discovery is that the band gap of the InGaN material system spans nearly the entire solar spectrum (0.7~3.4 eV), thus enabling design of multijunction solar cell structures with near ideal band gaps for maximum efficiency.

The figure shows the bang gap of several materials. For $In_xGa_{1-x}N$ material, the ratio of InN is x, and the ratio of GaN is 1-x(x = 0~1). Since it's a direct bandgap material, the bandgap of In $In_xGa_{1-x}N$ obey the following formula (1-1):

$$Eg_{\ InxGa1-xN} = 0.7 * x + 3.4 * (1-x)-1.43*x*(1-x) \qquad (1-1)$$

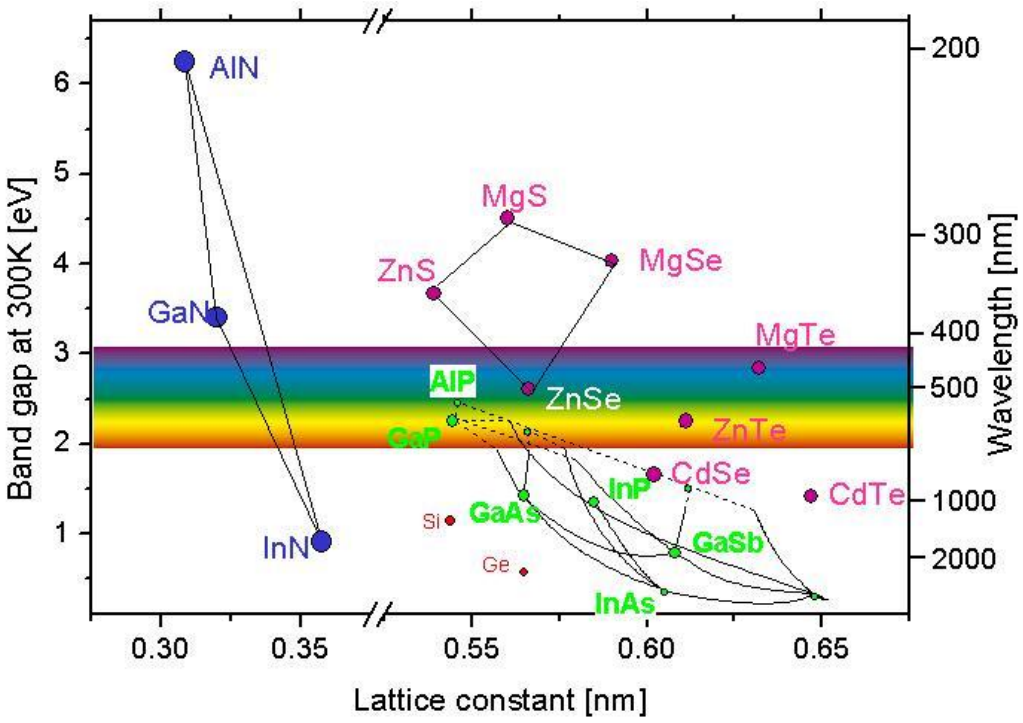

Figure 1.2-1 The bandgap and lattice constant of several materials.

1.2.2 The advantages and the challenge of GaN-Based solar cells

III-nitrides are ideally suited to the fabrication of optoelectronics devices such as lasers and light-emitting diodes, due to their high efficiency and wide applicability. The properties of III-nitrides include large carrier mobility, high drift velocity, strong optical absorption, and resistance to radiation, making them ideal for the development of photovoltaics.

Nowadays the p-GaN/i-InGaN/n-GaN heterojunction solar cells gets lots of attention because of some main advantages such as :

1. Direct band gap : Unlike Si-based solar cells, the band gap of GaN/InGaN is direct band gap. It means during the energy conversion, it won't loss some energy like heat. This point enhances the use of sunlight.

2. Tunable band gap : By mixing the different ratio of GaN/InGaN, we can have the band gap different from 0.7eV~3.4eV. The range is just overlap the solar spectrum. It means we can make the band gap just what we need.

This direct and wide band gap range makes the InGaN material system useful for photovoltaic applications due to the possibility of fabricating not only high-efficiency multijunction solar cells but also third-generation devices such as intermediate-band solar cells based solely on the nitride material system.

Despite the tremendous advantages and potential applications provided by GaN/InGaN solar cells, there still some challenges such as :

1. Growth of InGaN : The most important challenging task for high efficiency III-nitride solar cell is to grow high quality $In_xGa_{1-x}N$ materials with high In content. GaN is the most extensively studied material and comparatively has matured among the III-nitrides, while the lower band gap InGaN, which is more useful for photovoltaic application, is still a topic of fundamental research. High quality $In_xGa_{1-x}N$ layers with an In content from around 25 to 100% is required to obtain high-efficiency multijunction solar cells. Presently this becomes difficult with more than 20% content of Indium. Increasing the In content in InGaN during growth poses many challenges in controlling phase separation and defect density which results poor performances in the InGaN solar cells [7], [8], [9]. Growing an InGaN layer (>100 nm) with high crystal quality remains a challenge (Figure 1.2-2) and has severely limited the number of studies on p-GaN/i-InGaN/n-GaN heterojunction solar cells[10]-[13].

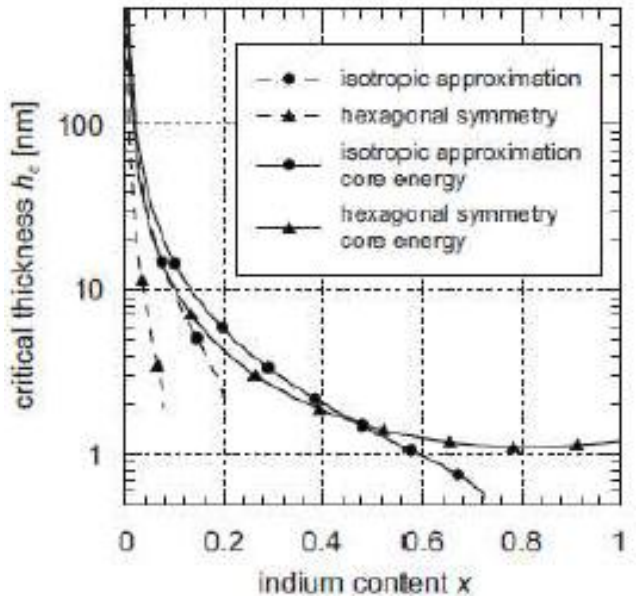

Figure 1.2-2 The relationship between critical thickness and indium content ratio.

2. Lattice mismatch and defects : The III-nitride solar cells face important challenges in lattice mismatch issue. The large difference in interatomic spacing between InN and GaN results poor quality growth of InGaN, especially in the intermediate range of In content . In general, a large lattice mismatch between InN and GaN and the low temperature growth of InGaN detracts from the crystalline quality in epitaxial layers and induces defects due to threading dislocation (TD), thereby generating nonradiative recombination centers (NRCs) in the light absorbing layer.[14] Furthermore, these defect centers trap and interact with photogenerated carriers, thereby reducing the carrier lifetime and short-circuit current carrier of the solar cells.[15]
3. Phase separation and In fluctuation and carrierdynamics : There are many roadblocks to achieving efficient III-nitride PV devices. Foremost, growing high quality InGaN layers with high indium compositions and the required thickness is difficult, which is already discussed. Phase separation in InGaN layer is also among the key challenges to obtain high performances solar cells. Phase separation is the

formation of microscopic or macroscopic domains of variable constituent composition in a material. Phase separation incorporates lower band gap domains within the material that absorbs corresponding low energy light, its effect is opposite to that of intermediate bands or quantum dots. As the size and distribution of the lower bandgap phase-separated domains are not optimal, they act as recombination centers decreasing the short circuit current of the solar cell. It is also evident from the theory of quantum well solar cells [16] that the lower bandgap material tends to dominate by pinning down the open circuit voltage of the device. When the thickness and/or mole fraction of InxGa1−xN materials increase, In-rich clusters in InGaN films easily induce phase separation. This leads to lower Voc compared with theoretical values, low FFs, and large recombination rate by defect states that degrade the Jsc of InGaN-based PV devices.

Although InGaN based solar cells offer tremendous potential for terrestrial as well as space photovoltaic applications, there are only a few reports on InGaN based solar cells. Furthermore, most reported InGaN solar cells have In contents lower than 15% and band gaps near 3 eV, or larger, and therefore deliver diminishing quantum efficiency at wavelengths longer than 420 nm.[17]-[21] An earlier theoretical material system to obtain solar cells having a solar energy conversion efficiency greater than 50% can be fulfilled by InGaN alloys with In content of about 40%.[22] Additionally, III-nitride multijunction solar cells with near ideal band gaps for maximum solar energy conversion efficiency must incorporate InGaN layers with higher In contents or lower energy band gaps. However, the realization of high crystalline quality In- GaN films in the entire composition range is highly challenging. One of the biggest problems is attributed to the large lattice mismatch between InN and GaN, resulting in low solubility and phase separation.[23]-[24]

InGaN/GaN multiple quantum well solar cells is one way to improve lattice mismatch and critical thickness. In this way, we can grow higher In content layer with short thickness in

order to enhance the absorption of the incident light.

1.3 Motivation

The high efficiency solar cells has become more and more important in the future. Compared to Silicon-based solar cell, the GaN solar cell has higher efficiency and is considered for future generation of photovoltaics applications. But due to the absorption range of GaN/InGaN solar cells is short, otherwise the reflectance of GaN is over 20% without any antireflection coating layer. So how to achieve the most use of the light will be an important issue in GaN/InGaN solar cells.

So antireflection is a key technique for efficiently harvesting solar photon. Several studies of nanostructure demonstrate it offer ultra-low reflectivity.

As mentioned before, the absorption range for GaN/InGaN solar cells is short. So how to use the short wavelength region is an important thing to enhance the efficiency of InGaN/GaN multiple quantum well solar cells. We observe the ITO will absorb the the light before 380nm. That will cause a big loss.

In this study we will compare the flat InGaN/GaN multiple quantum well solar cells to the nanostructured ones. We used textured PDMS film to reduce the reflectance without making electricity property poor. We use a material called quantum dots (QDs) to solve the problem of high absorption of front ITO layer. QDs will absorb the short wavelength light before ITO and reemit the visible region light. So we can reduce the UV region light loss.

Chaper 2. Basic Theories of Solar Cell

2.1 The fundamental structure of solar cell

A complete solar cell structure design was shown in Figure 2.1-1 [25]-[26], there is a glass protective layer (cover glass) and a transparent adhesive layer outside, which play the role of fixed and the protection of the internal components of solar cells are not damage by the environment water vapor and other material. According to their function the internal components of solar cell, they can be divided into three parts, the first one is the anti-reflective layer (antireflection coating), which improve the light harvesting in solar cell by the optical design further to reduce optical losses due to the reflection; The second one is the semiconductor pn junction (active layer), the pn junction can absorb the light and generate the electron-hole pair and then separate the electron and hole which diffuse to the electric field the between the pn junction. The third one is electrode, which extract the carrier. The front electrode which allows light to pass through so it will be designed into different spacing and the rate of metal shielding finger patterns according to different cells, back electrode which with the whole plane structure, and reflect the light which one is incomplete absorbed at once optical path back to the active layer and increase the power conversion efficiency. By using the load of outside circuit, the photocurrent can change into to an output power. For enhancing the power efficiency of solar cell, there are three keys can be improved.

(i) Enhancing the photon collection, the implementation is an anti-reflective layer, an effective anti-reflective layer in solar cells which should have features of broadband and omnidirectional anti-reflective characteristics, and increase the photo collection per unit area of solar cells.

(ii) Enhancing the internal quantum efficiency (IQE), the implementation is improving the quality of semiconductor material. Reducing the semiconductor

material defect at manufacturing process or reducing opportunity of the carrier recombines by defect. Developing high-quality solar material or by epitaxial process to create the most suitable structure for photovoltaic which improve the solar energy conversion efficiency and has a broadband absorption spectrum.

(iii) Enhancing the electron extraction (Carrier collection), the implementation is to develop a high-quality electrodes. The front electrode which allows light to pass through, it will be designed into different spacing and the rate of metal shielding finger patterns according to different cells further to enhance the electron extraction. Another key point of electrode design is reducing the series resistance and forms an ohmic contact to reduce the loss of carrier.

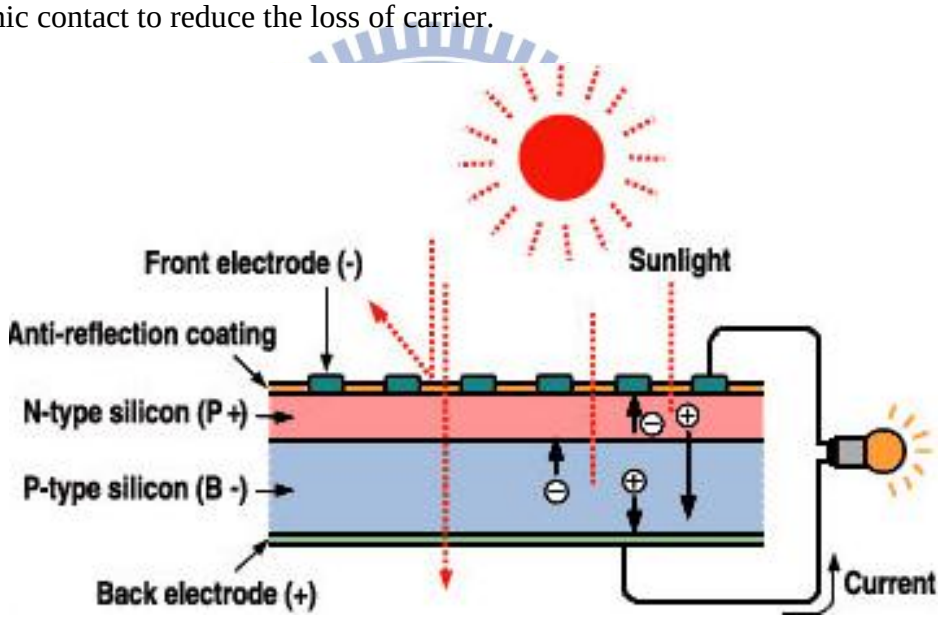

Figure 2.1-1 Illustrations of the fundamental structure of solar cell

2.2 The physics of solar cells

Typically, solar cell was formed as a diode, and there is a pn junction between the n-type and p-type semiconductor, due to the different concentration of electron and hole, carrier diffusion will occur and result in diffusion current. In the vicinity of the junction, the electron concentration of n-type is higher than the electron concentration in p-type, so the electron will diffuse form n-type to p-type. Similarly, the hole concentration of p-type is

higher than the hole concentration in n-type, so the hole will diffuse form p-type to n-type, so the neutral will be broken. The junction at the n-type side will exist the positive charges which were caused by the donor, and the junction at the p-type side will exist the negative charges which were caused by the acceptor. The region with n-type positive charges and p-type negative charges which we called space charge region, and there is an electrical field in the space charge region and the direction is from n-type side to p-type side.

When the light with the energy higher than the band gap of the semiconductor was incident, the light will be absorbed then transfer the energy to electrons, and then the electron are excited to a higher energy state which resulting in an electron - hole pairs. Due to the built-in electrical fields the electrons will move to the n-type region and the holes will move to the p-type region. The electron hole pairs move by the built-in electrical fields will result in drift current.

The basic working principle of solar cells is separate the electron hole pairs by using the built-in electrical field in the space charge region before they recombine. Figure 2.2-1 shows the diffusion mechanism and drift mechanism when the light incident into the solar cell, the photocurrent is the sum of diffusion current and drift current [27]-[28]. If we make a contact with two terminals in a diode, it is called short circuit and the current was called short circuit current which equal to photocurrent. If there is no contact with two terminals in a diode, it is called open circuit, when the light incident, the electron will accumulate at n-type side and the hole will accumulate at p-type side which results in a photo-voltage or called open circuit voltage.

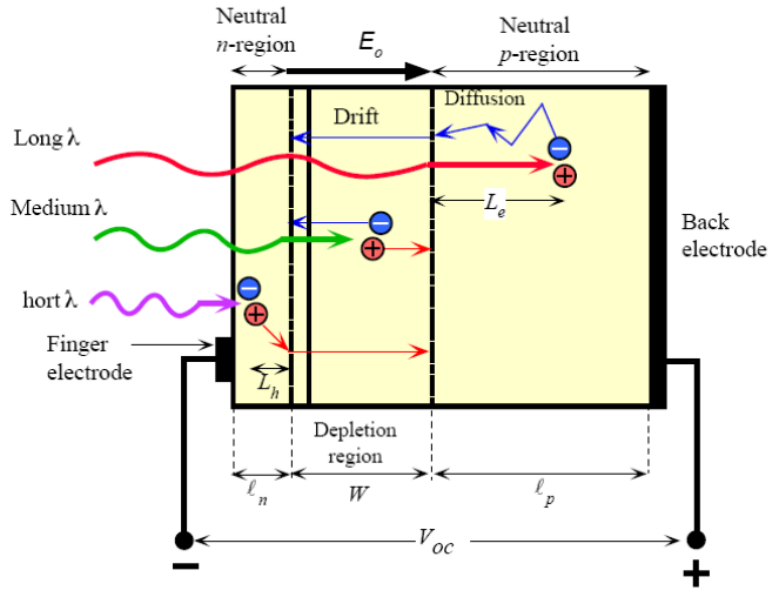

Figure 2.2-1 Illustrations of the carrier generation, carrier diffusion and carrier drift in solar cell

2.3 The parameter of solar cells

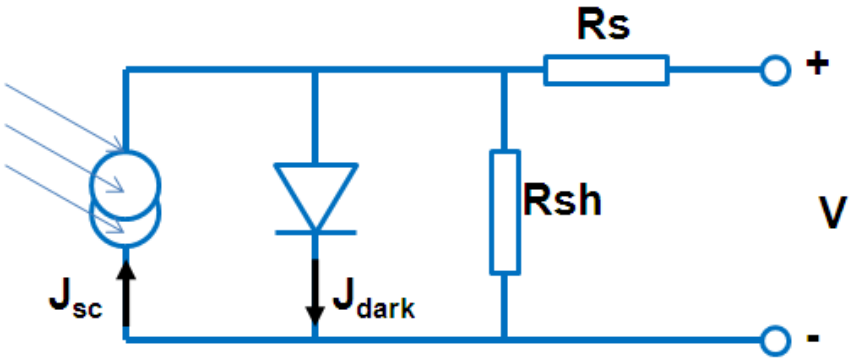

Figure 2.3-1 The diagram of solar cell equivalent circuit.

Figure 2.3-1 illustrates the equivalent circuit of solar cell. From this diagram, one could find the photo-generated current (I) as follows [29]:

$$I = I_{sc} - I_0\left\{\exp\left[\frac{q(V+IR_S)}{nkT}\right] - 1\right\} - \frac{V+IR_S}{R_{sh}} \quad (2\text{-}1)$$

where I_{sc} is the short-circuit current (also called light-generated current, I_L), I_0 is the reverse saturation current of the diode, k is the Boltzmann's constant, T is the absolute temperature in

degrees Kelvin, n is the ideality factor of diode ($1 < n < 2$, n=1 for the Shockley equation), R_s is the equivalent series resistance and R_{sh} is the equivalent shunt resistance of the solar cell. An idealized solar cell, the series resistance R_s is close to infinity and treats as open in the equivalent circuit. Therefore, the Eq. (2-1) can simplified as:

$$I = I_{sc} - I_0 \left[\exp\left(\frac{qV}{nkT}\right) - 1\right] \quad (2\text{-}2)$$

In Figure 2.3-1, when the intensity of solar radiation is weak, the current of diode is approximately the leakage current ($I_d \approx \frac{V_d}{R_{sh}}$), therefore, R_s can be ignore and R_{sh} effect is important, then Eq. (2-1) can be rewritten as:

$$I = I_{sc} - I_0 \left[\exp\left(\frac{qV}{nkT} - 1\right)\right] - \frac{V}{R_{sh}} \quad (2\text{-}3)$$

When the intensity of solar radiation is great, the light-generated current is great and diode is on condition. Therefore, the current of diode is greater than the leakage current ($I_d \gg \frac{V_d}{R_{sh}}$), and the Rsh can be ignore and the Rs effect is important. Then the Eq. (2-1) can be rewritten as:

$$I = I_{sc} - I_0 \left[\exp\left(\frac{qV+IR_s}{nkT}\right) - 1\right] \quad (2\text{-}4)$$

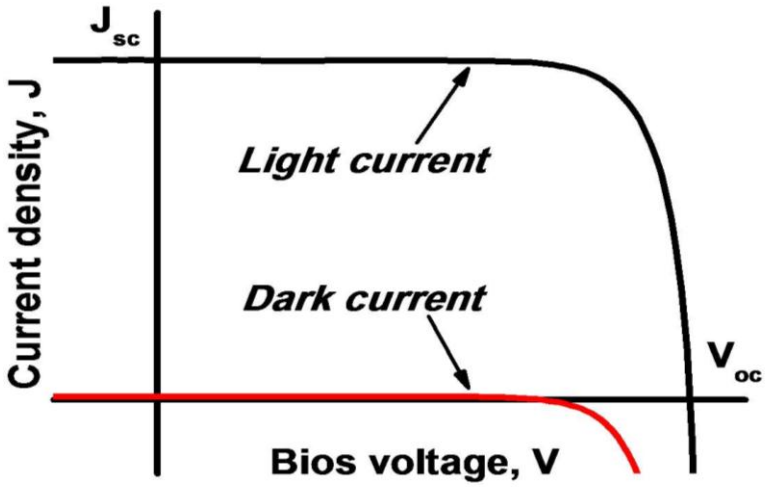

Figure 2.3-2 The I-V characteristics with and without illumination.

The I-V characteristics of solar cell in dark condition and under illumination were shown in Figure 2.3-2 [30]. Four parameters are usually used to characterize the solar cell output performances and shown in this figure. The parameters used to describe the solar cell performances are indicated as follows [31]:

(1) Short-Circuit Current, I_{sc}

I_{sc} is a current when the solar cells were under illumination, and with a zero external load, it means the solar cell circuit is short circuit. It is determined on the voltage (V) equal to zero by Eq. (2-2). This is equal to the light-generated current I_L ideally. As V=0, the Eq. (2-2) can be written as:

$$I = I_{sc} \tag{2-5}$$

(2) Open-Circuit Voltage, V_{oc}

The open-circuit voltage is is a voltage when the solar cells were under illumination, and with an infinite external load, it means the solar cell circuit is open circuit, at this time the output current is zero. V_{oc} can be solved in I=0 and V=V_{oc} from Eq. (2-2), which is expressed as:

$$V_{oc} = \frac{nkT}{q}\ln\left(\frac{I_{sc}}{I_0} + 1\right) \tag{2-6}$$

V_{oc} is determined by the properties of the semiconductor by virtue of its dependence on I_0.

(3) Fill Factor, FF

Which is defined as the maximum ratio of the output power to the product on the short-circuit current and open-circuit voltage, which can be expressed as:

$$FF \equiv \frac{I_{max}\times V_{max}}{I_{sc}\times V_{oc}} = \frac{P_{max}}{I_{sc}\times V_{oc}} = 1 - \frac{kT}{qV_{oc}}\ln\left(1 + \frac{qV_{max}}{kT}\right) - \frac{kT}{qV_{oc}} \tag{2-7}$$

It is measure of how squareness the output characteristics are. For cell of reasonably efficiency, it has a value in the range 0.7 to 0.85.

(4) Conversion Efficiency, η

The conversion efficiency of solar cell is defined as the maximum ratio of the output power to the input power, which can be expressed as

$$\eta = \frac{P_{max}}{P_{in}} = \frac{I_{max} \times V_{max}}{P_{in}} = \frac{I_{sc} \times V_{oc} \times FF}{P_{in}} = \frac{I_L \times \left[1 - \frac{kT}{qV_{oc}} \ln\left(1 + \frac{qV_{max}}{kT}\right) - \frac{kT}{qV_{oc}}\right]}{P_{in}} \qquad (2\text{-}8)$$

where P_{in} is the total power under the light incident to the cell.

The solar cell parameters such as open-circuit voltage V_{oc}, short-circuit current I_{sc} and fill factor FF can provide the information about designing and improving the photodiode due to their characteristics depended on the properties of the semiconductor materials and the structure of device.

(5) Quantum Efficiency

Quantum efficiency (QE) is the ratio of the number of charge carriers collected by the solar cell to the number of photons of a given energy shining on the solar cell. QE therefore relates to the response of a solar cell to the various wavelengths in the spectrum of light shining on the cell. The QE is given as a function of either wavelength or energy. If all the photons of a certain wavelength are absorbed and we collect the resulting minority carriers (for example, electrons in a p-type material), and then the QE at that particular wavelength has a value of one. The QE for photons with energy below the band gap is zero.

The quantum efficiency ideally has a square shape, where the QE value is fairly constant across the entire spectrum of wavelengths measured. However, the QE for most solar cells is reduced because of the effects of recombination, where charge carriers are not able to move into an external circuit. The same mechanisms that affect the collection probability also affect

the QE. For example, modifying the front surface can affect carriers generated near the surface. And because high-energy (blue) light is absorbed very close to the surface, considerable recombination at the front surface will affect the "blue" portion of the QE. Similarly, lower energy (green) light is absorbed in the bulk of a solar cell, and a low diffusion length will affect the collection probability from the solar cell bulk, reducing the QE in the green portion of the spectrum. In somewhat technical terms, the quantum efficiency can be viewed as the collection probability due to the generation profile of a single wavelength, integrated over the device thickness and normalized to the number of incident photons.

"Quantum efficiency" is also sometimes called IPCE, which stands for Incident-Photon-to-electron Conversion Efficiency.

Two types of quantum efficiency (QE) of a solar cell are often considered:

- External Quantum Efficiency (EQE) is the ratio of the number of charge carriers collected by the solar cell to the number of photons of a given energy shining on the solar cell from outside (incident photons).
- Internal Quantum Efficiency (IQE) is the ratio of the number of charge carriers collected by the solar cell to the number of photons of a given energy that shine on the solar cell from outside and are absorbed by the cell.

The IQE is always larger than the EQE. A low IQE indicates that the active layer of the solar cell is unable to make good use of the photons. A low EQE can indicate that, but it can also, instead, indicate that a lot of the light was reflected.

To measure the IQE, one first measures the EQE of the solar device, then measures its transmission and reflection, and combines these data to infer the IQE.

(6) Parasitic Resistances

In real cells power is dissipated through the resistance of the contacts and through leakage currents around the sides of the device. These effects are equivalent electrically to two parasitic resistances in series (R_s) and in parallel (R_{sh}) with the cell (Figure 2.3.3).

The series resistance arises from the resistance of the cell material to current flow, particularly through the front surface to the contacts, and from resistive contacts. Series resistance is a particular problem at high current densities, for instance under concentrated light. The parallel or shunt resistance arise from leakage of current through the cell, around the edges of the device and between contacts of different polarity. It is a problem in poorly rectifying devices.

Series and parallel resistance reduce the fill factor as shown in Figure 2.3-3. For an efficient cell we want R_s to be as small and R_{sh} to be as large as possible.

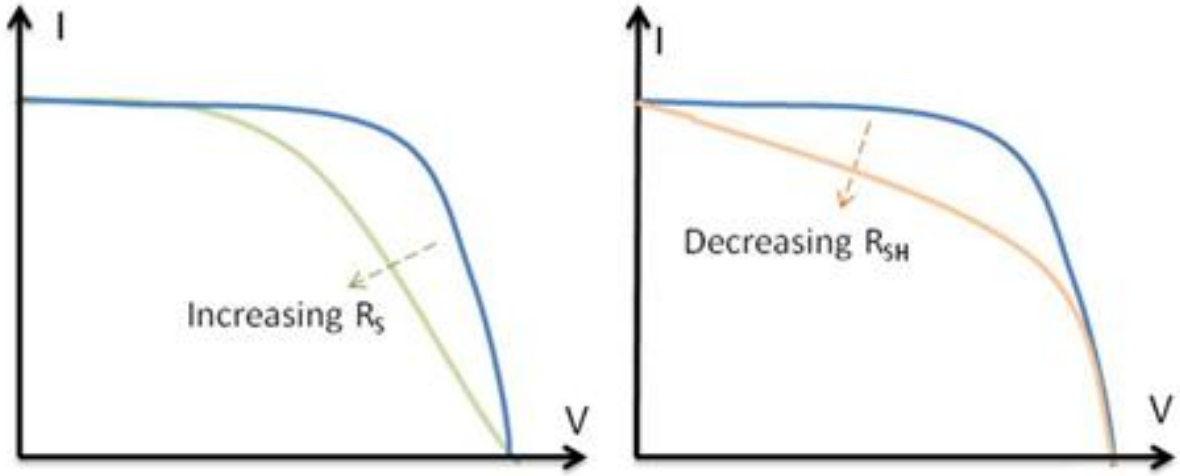

Figure 2.3-3 Effect of increasing series and reducing parallel resistances. In each case the outer curve has $R_s = 0$ and $R_{sh} = \infty$. In each case the effect of the resistances is to reduce the area of the maximum power rectangle compared to $J_{sc} \times V_{oc}$.

Chaper 3. Experimental Instruments and Measuring Instruments

3.1 Scanning Electron Microsope (SEM)

A scanning electron microscope (SEM) is a type of electron microscope that images a sample by scanning it with a high-energy beam of electrons in a raster scan pattern. The electrons interact with the atoms that make up the sample producing signals that contain information about the sample's surface topography, composition, and other properties such as electrical conductivity.

The types of signals produced by an SEM include secondary electrons, back-scattered electrons (BSE), characteristic X-rays, light (cathodoluminescence), specimen current and transmitted electrons. Secondary electron detectors are common in all SEMs, but it is rare that a single machine would have detectors for all possible signals. The signals result from interactions of the electron beam with atoms at or near the surface of the sample. In the most common or standard detection mode, secondary electron imaging or SEI, the SEM can produce very high-resolution images of a sample surface, revealing details less than 1 nm in size. Due to the very narrow electron beam, SEM micrographs have a large depth of field yielding a characteristic three-dimensional appearance useful for understanding the surface structure of a sample. This is exemplified by the micrograph of pollen shown to the right. A wide range of magnifications is possible, from about 10 times (about equivalent to that of a powerful hand-lens) to more than 500,000 times, about 250 times the magnification limit of the best light microscopes. Back-scattered electrons (BSE) are beam electrons that are reflected from the sample by elastic scattering. BSE are often used in analytical SEM along with the spectra made from the characteristic X-rays. Because the intensity of the BSE signal is strongly related to the atomic number (Z) of the specimen, BSE images can provide information about the distribution of different elements in the sample. For the same reason, BSE imaging can image colloidal gold immuno-labels of 5 or 10 nm diameter which would

otherwise be difficult or impossible to detect in secondary electron images in biological specimens. Characteristic X-rays are emitted when the electron beam removes an inner shell electron from the sample, causing a higher energy electron to fill the shell and release energy. These characteristic X-rays are used to identify the composition and measure the abundance of elements in the sample [32].

As the sample is scanned by the electron beam as shown in figure 3.1-1, it emits electrons and electromagnetic radiation. A detector counts the low energy secondary electrons (< 50 eV) or other radiation emitted. The image is produced by two dimensional intensity distributions by scanning a cathode ray tube (CRT) spot onto a screen and modulating the brightness by the amplified current from the detector. Three dimensional samples change the way electrons are emitted and results in the appearance of a three dimensional image. Resolutions less than 1 nm may be achieved.

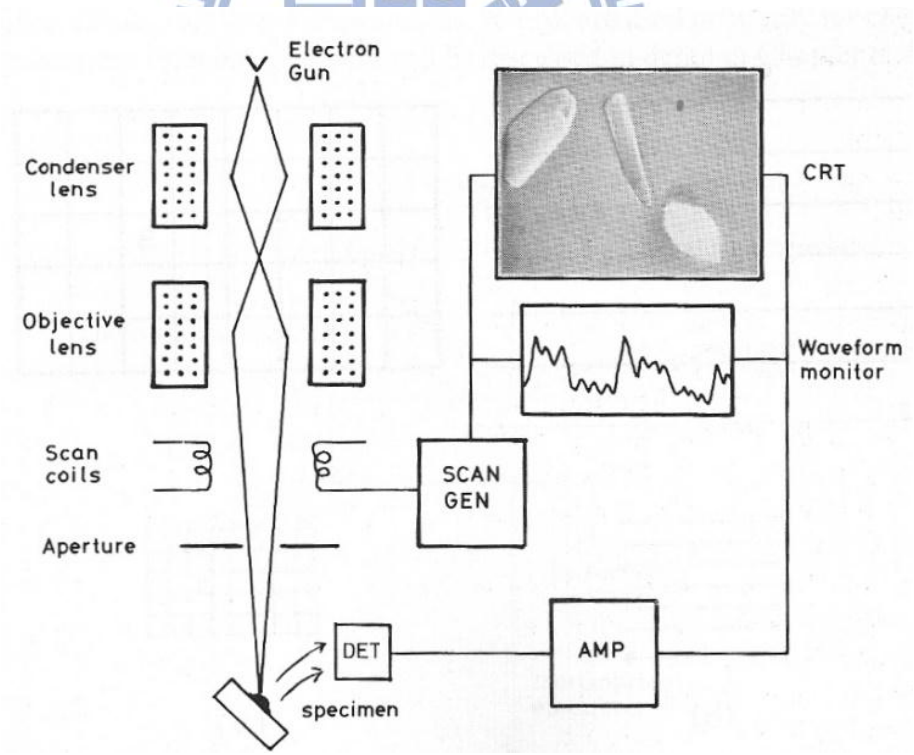

Figure 3.1-1 Schematic diagram of a scanning electron microscope.

3.2 Plasma-enhanced chemical vapor deposition (PECVD)

Plasma-enhanced chemical vapor deposition (PECVD) is a process used to deposit thin films from a gas state (vapor) to a solid state on a substrate. Chemical reactions are involved in the process, which occur after creation of a plasma of the reacting gases. The plasma is generally created by RF (AC) frequency or DC discharge between two electrodes, the space between which is filled with the reacting gases.

Plasma deposition is often used in semiconductor manufacturing to deposit films onto wafers containing metal layers or other temperature-sensitive structures. Silicon dioxide can be deposited from dichlorosilane or silane and oxygen, typically at pressures from a few hundred millitorr to a few torr. Plasma-deposited silicon nitride, formed from silane and ammonia or nitrogen, is also widely used, although it is important to note that it is not possible to deposit a pure nitride in this fashion. Plasma nitrides always contain a large amount of hydrogen, which can be bonded to silicon (Si-H) or nitrogen (Si-NH); this hydrogen has an important influence on UV absorption, stability, mechanical stress, and electrical conductivity.

Silicon Dioxide can also be deposited from tetraethoxysilane (TEOS) in an oxygen or oxygen-argon plasma. These films can be contaminated with significant carbon and hydrogen as silanol, and can be unstable in air. Pressures of a few torr and small electrode spacings, and/or dual frequency deposition, are helpful to achieve high deposition rates with good film stability.

High-density plasma deposition of silicon dioxide from silane and oxygen/argon has been widely used to create a nearly hydrogen-free film with good conformality over complex surfaces, the latter resulting from intense ion bombardment and consequent sputtering of the deposited molecules from vertical onto horizontal surfaces [33].

3.3 Inductively-Coupled Plasma (ICP)

ICP etching system is dry etching system. The plasma region was crylindrical. This low aspect ratio contributes to the high plasma production efficiency in that it reduced the ratio of the plasma flux hitting the walls to the plasma flux hitting to the wafer. A circular array of magnetic line cusps was used to aid in plasma confinement and improve uniformity. The plasma was driven by a coil, separated from the plasma by a dielectric window.

The plasma-assisted etching process proceeds in five steps as illustrated in Figure3.3-1.

1. The process began with the generation of the etchant species in the plasma.
2. The reactant was transported by diffusion through a stagnant gas layer to the surface.
3. The reactant was adsorbed to the surface.
4. This was followed by chemical reaction along with physical effects, such as ion bombardment to form volatile compounds.
5. These compounds were desorbed from the surface, diffused into the bulk gas, and pumped out by the vacuum system.

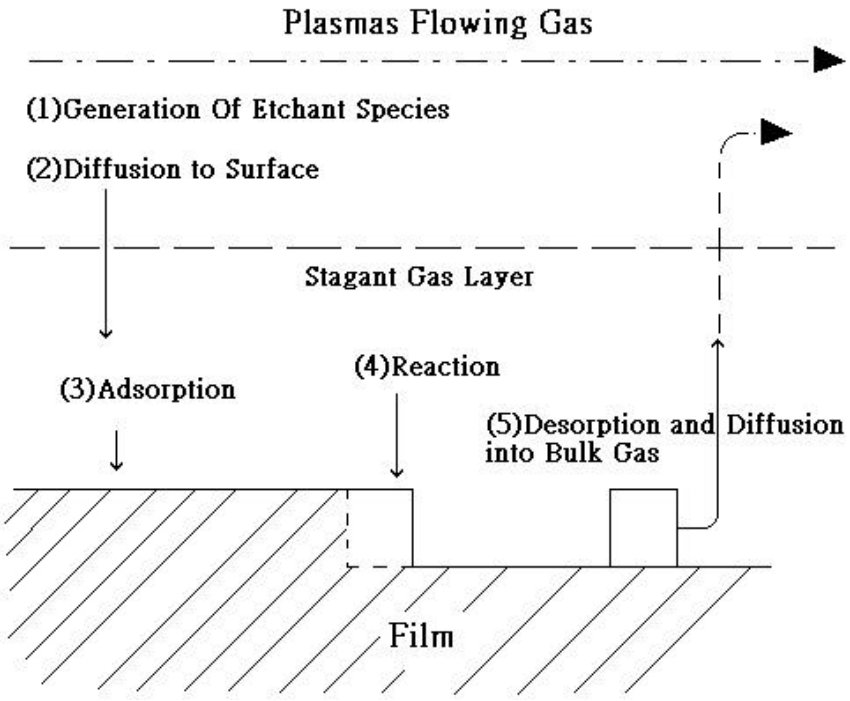

Figure 3.3-1 The plasma-assisted etching process proceeds

Here we use nanosphere spreaded on GaN to be mask etching by ICP-RIE to form some nanostructure. We use Cl_2/Ar to be the etching gas. By adding different ratio of the gas, we can achieve different kinds of the nanoscale shape.

3.4 Current-voltage measurement (J-V curve)

Solar cell device characteristics measurement and analysis in the laboratory, set up by self-complete measure machine architecture to achieve. We use the U.S. company manufacturing Newport's AM1.5G 1000W Class A standard solar simulator, the United States National Renewable Energy Laboratory (NREL) calibrated with international standards set by the solar spectrum in all bands are within error of only 2%. Before the actual measurement, using Newport calibration with standard solar cells go after the correction light intensity under the conditions in 1 sun. We use the temperature controller to maintain the temperature of load placed at 25℃. And with a Keithley 2400 digital power meter, through a computer Labview program to control the I-V measurement system. Figure 3.4-1 is our measuring machine architecture:

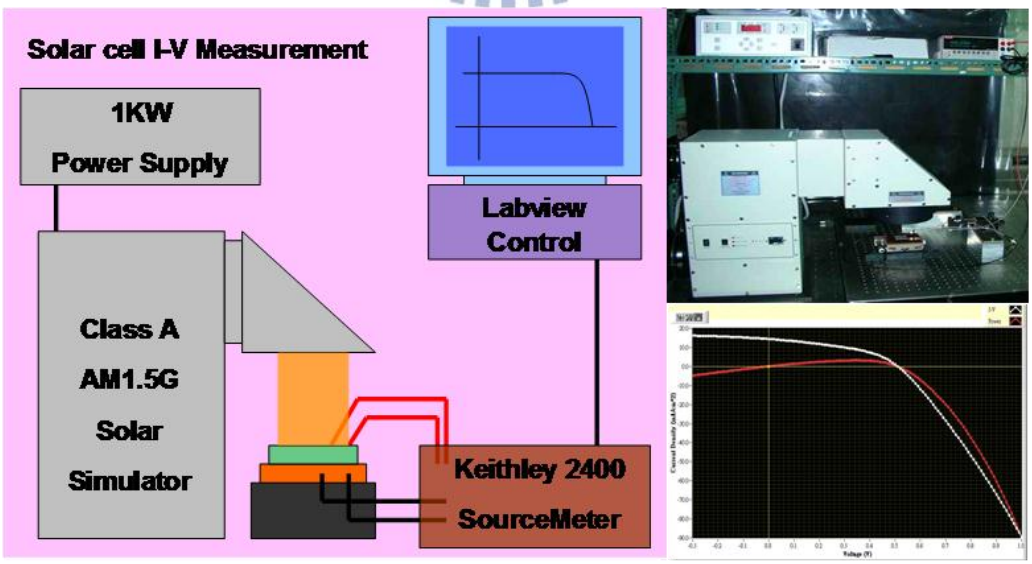

Figure 3.4-1 The schematic of Current-voltage measurement system

Energy conversion efficiency of solar cells is measured the I-V characteristics under simulated sunlight illumination conditions (AM1.5G). We can learn about the important parameters through the conversion efficiency of solar cells, including short-circuit current (I_{sc}), open-circuit voltage (V_{oc}), fill factor (FF), power conversion efficiency (η), Maxima power voltage (V_{max}), Maxima power current (I_{max}), series resistance (R_s), and shunt resistance (R_{sh}).

3.5 External quantum efficiency measurement (EQE)

Measuring the external quantum efficiency (QE (λ)), also known as spectral response (SR (λ)) is very important for understanding the carrier generation and the diffusion mechanism of photovoltaic device. The unit of spectral is the amperage of current generate from per wattage of incident light (A / W). Formula 3-1 shows the mathematical formula of external quantum efficiency, which indicate the probability of incident photon transform to electron-hole pairs.

$$QE(\lambda) = \frac{qSR(\lambda)}{\lambda hc} \tag{3-1}$$

We assume that the operating point of maximum power output and short-circuit are the same, so usually the spectral response is the short circuit current. During solar cell research there are several systems of external quantum efficiency measurement, such as interference filter, grating spectrometer etc... For single-junction solar cells we use the periodic single-frequency light to irradiate solar cell and measure the photocurrent then using lock-in amplifier to transfer the signal into AC signal. In our experiment we use a grating spectrometer system for broadband spectral measurements (400-3200 nm) and for high spectral resolution, the setup is as figure 3.5-1 [34]. Xenon lamp with wide spectrum when the wide spectrum light pass through a grating it will become a single frequency light and then focus on the solar cell. The aberration can be solved by using a spherical mirror or a parabolic mirror.

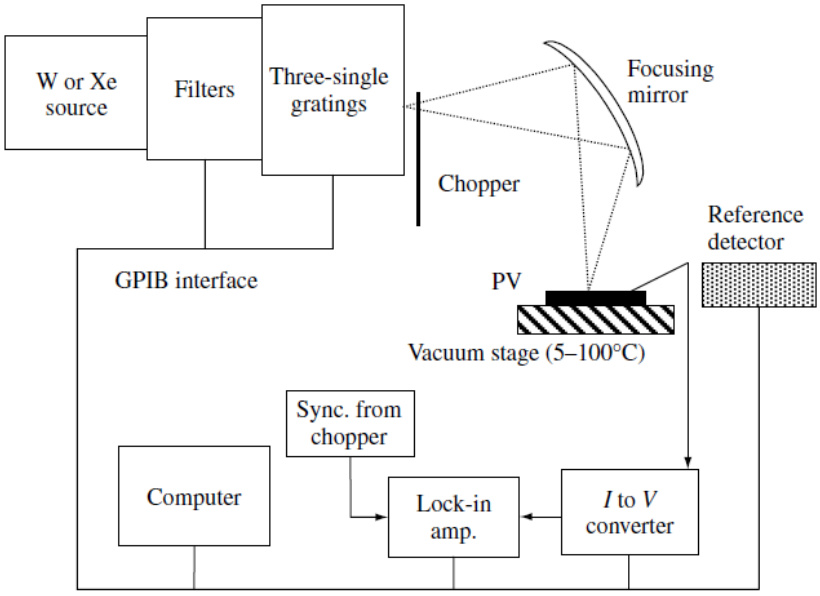

Figure 3.5-1 The schematic of grating quantum efficiency measurement system

3.6 Angle resolved Integrating sphere reflectance measurements

Figure 3.6-1(a) is a traditional reflectivity measurements diagram. When we want to measure the reflectance of the smooth surface, the laser light is incident to the sample surface by a specific angle. As the sample itself is a smooth surface, and the incident light is single wavelength, we can obtain the reflected light at corresponding angle by the Snell's law. At this point we just put on a light detector on the path of the reflected light, and we can collect the reflected light from the sample surface effectively. Thus it can measure the reflectance value.

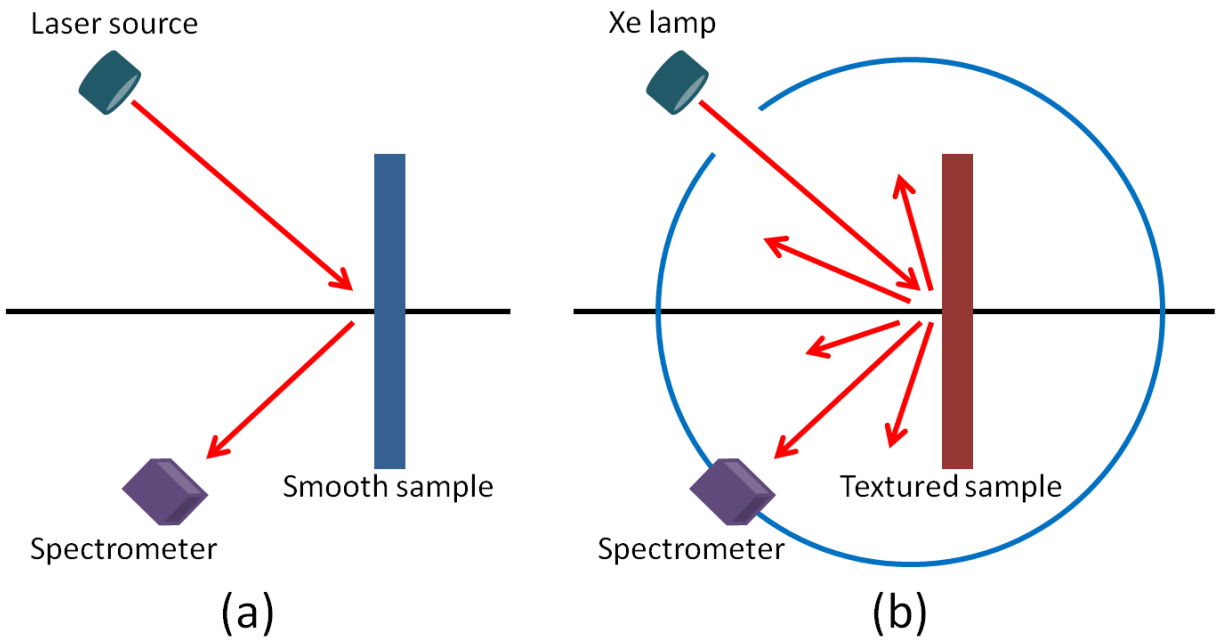

Figure 3.6-1 (a) Schematic diagram of conventional reflectivity measurements. (b) Schematic diagram of Integrating sphere reflectance measurements.

For the particles surface or rough samples, we also want to understand the different wavelengths light reflectivity, so we change the incident light source to the Xe lamp light with broadband spectrum. Figure 3.6-1(b) shows, when we made the surface of the textured structure which the dimension size is closed to the wavelength of incident light, the different wavelengths of light on the structure surface produce different levels of splitting, and at the same time with a large number of light diffraction and scattering phenomenon, which will make the direction of reflected light is no longer regularly, but from different angles toward the divergent out. In such condition, if we still use previously measurement way which placed a light detector in a particular direction, we will only receive a small portion of the reflected light, so that out of the reflectance measurement is not an objective value. For rough surface samples, in order to improve the problem of not only received light at a specific point, Fig. 3.6-1(b), our approach is coupled with an integrating sphere to collect the complete angle scatter light, the light spilling in all directions will be limited to points inside the integrating

sphere and were eventually collected by the light detector. And in order to analyze the reflectivity of different wavelengths, we require a light detector which can detect wide spectrum of light. By this way we obtained an objective of the reflectivity data, which compared to the previous method of measuring reflectivity will be more realistic and accurate.

Figure 3.6-2 you can see the whole device roughly, we use Xe lamp as the light source to simulate a wide spectrum of solar incident light, then light pass a convex lens by a guiding fiber, this allows light to show about horizontal to pass the aperture of the integrating sphere.

The horizontal light pass the aperture of the integrating sphere then illuminate the sample on the fixture in the integrating sphere. The reflected light is not absorbed by the sample will be limited to points inside the integrating sphere, and then be collected by the light detector at the rear of integrating sphere. This fixture platform can be set around rotating, and we can use this rotating to change the incident light angle of sample illumination. So the angle-resolved reflection of textured sample can be measured by the integrating sphere easily.

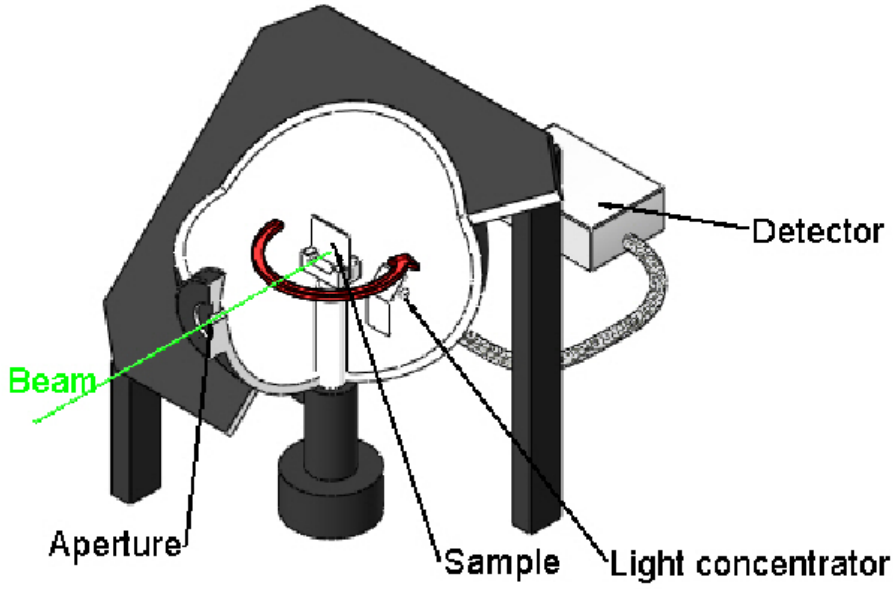

Figure 3.6-2 Schematic diagram of integrating sphere in our laboratory.

Chaper 4. Device fabrication and characteristics analysis

4.1 The fabrication of GaN/InGaN multiple quantum well solar cells

Figure 4.1-1 shows the fabrication flows of GaN/InGaN multiple quantum well solar cells. As mentioned before, GaN/InGaN multiple quantum well solar cells is better than bulk i-layer because we can grow higher content indium with thin thickness. So we decide to use this type to grow our solar cell. The p-GaN 、 i-layer (GaN/InGaN multiple quantum well)、n-GaN was deposited by Metal-organic Chemical Vapor Deposition (MOCVD) on sapphire substrate. Then we use Plasma-enhanced chemical vapor deposition (PECVD) to grow SiNx(Figure 4.1-1 (a)). After that, we use mask aligner and exposure system to define mesa pattern and the Photo Resistor (PR) was used as mask immersed in Buffered Oxide Etch (BOE) to remove some SiNx. Then we remove the rest PR by Acetone. The sample was etching by Inductively-Coupled Plasma (ICP) with SiNx as mask. The p-n junction was defined as figure 4.1-1(b). Then we use sputter to grow Indium tin oxide(ITO). After that, we use mask aligner and exposure system to define ITO pattern and the PR was used as mask immersed in aqua regia to remove some ITO(figure 4.1-1(c)). And the ITO on p-GaN was used as Transparent conductive layer. Then we use mask aligner and exposure system to define electrode pattern. We use E-gun to deposit our electrode. After that, we remove the PR in acetone. Finally, the GaN/InGaN multiple quantum well solar cells is achieved. (figure 4.1-1(d)) The material and the thickness are in following tables.

Substrate	p-type	Active layer	n-type	Conducting layer	electrode
sapphire	p-GaN	i-GaN/InGaN	n-GaN	ITO	Cr
430um	200nm	112nm	1.5um	110nm	50nm

Table 4.1-1 The content and the thickness of our GaN/InGaN multiple quantum well solar cells

i-layer	content	thickness	In (%)
Quantum well	14pair GaN/InGaN	5nm/3nm	16%

Table 4.1-2 The content and the thickness of i-layer.

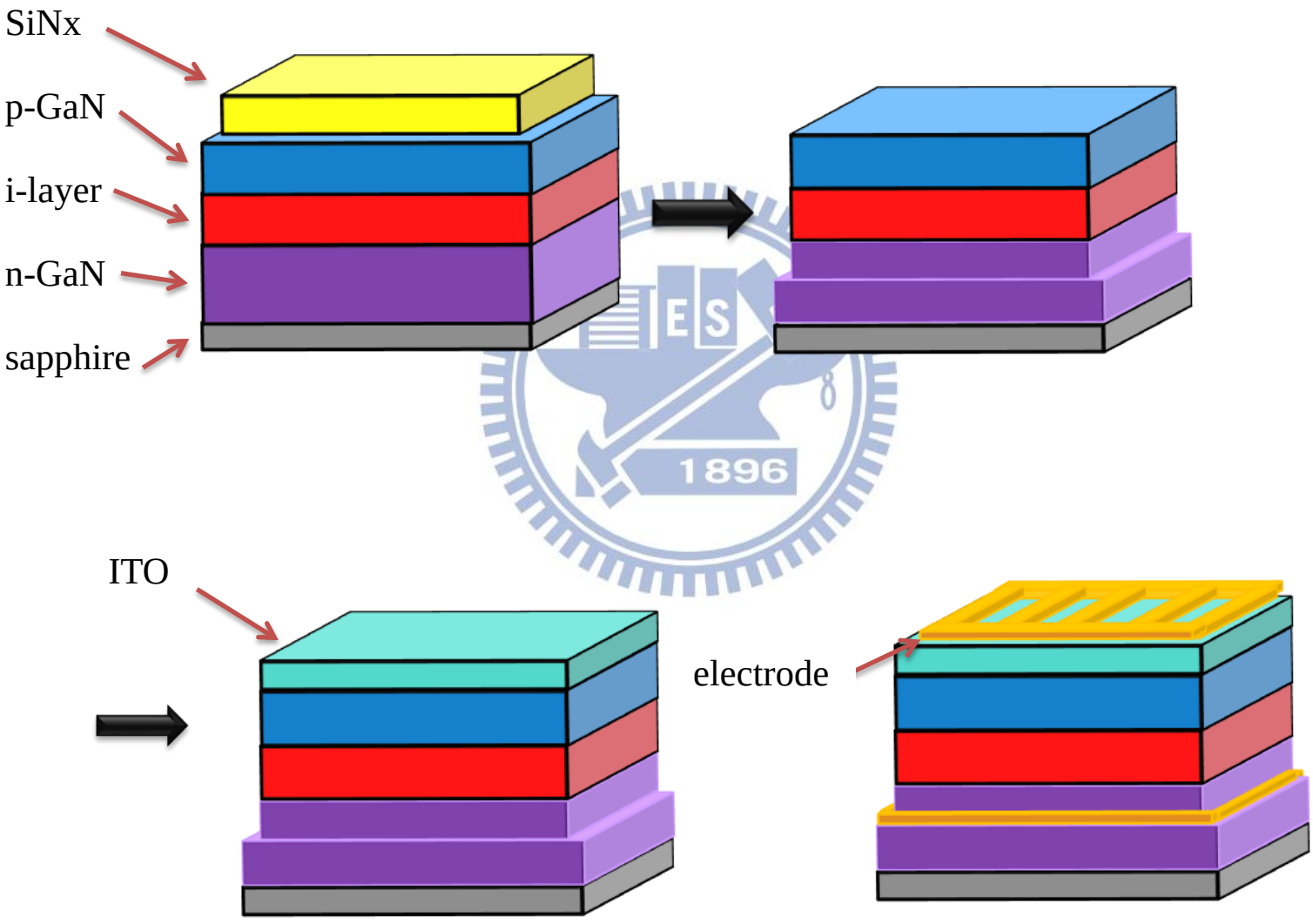

Figure 4.1-1 The fabrication flows of GaN/InGaN multiple quantum well solar cells.

4.2 Polydimethylsiloxane (PDMS)

Due to lots of defects caused by the dry etching process mentioned before, the electricity properties must be poor. These defects will trap the electron-hole and decrease the efficiency. So we found another material to reduce the Fresnel reflection which called Polydimethylsiloxane (PDMS). The advantages of using PDMS film are the low-cost, non-vacuum system and simple process (only spin coating and imprinting needed). Other than ease of fabrication, PDMS film provides a refractive index gradient to serve as an anti-reflection layer. Extra benefits of light trapping and scattering can be added when the film is stamped with high texture pattern.

4.2.1 Fabrication process of textured PDMS film

To prepare a flexible textured PDMS film, a randomly textured crystalline silicon (c-Si) mold-pattern was prepared by wet-etching with potassium hydroxide (KOH) [35]-[36], which was used to imprint PDMS film(figure 4.2.1-1(a)), and the cross-sectional scanning electron microscope (SEM) image of the randomly textured silicon substrate with a height of about 6 μm was shown Fig. 4.2.1-2(a). Second, the PDMS pre-polymer solution (in the form of a viscous liquid) was dropped on randomly textured c-Si mold-pattern surface. Then, the spin coating method was employed to form a uniformly PDMS polymer layer which can cover over the c-Si mold-pattern(figure 4.2.1-1(b)), and then the substrate was baked at 70 ℃ for half hour. After detaching from the c-Si mold, a flexible textured PDMS film was successfully obtained(figure 4.2.1-1(c)) and the height of the textured structure was about 3 μm, as shown in Fig. 4.2.1-2 (b). Finally, the flexible textured PDMS film was put on the cell(figure4.2.1-3).

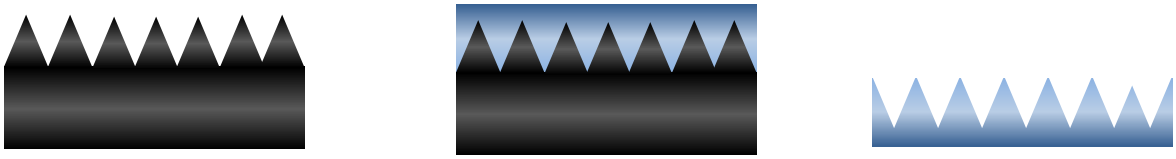

(a) (b) (c)

Figure 4.2.1-1 The fabrication flows of rough PDMS film. Figure (a) is the textured substrate. Figure(b) is the PDMS spread on the substrate. Figure (c) is the rough PDMS film.

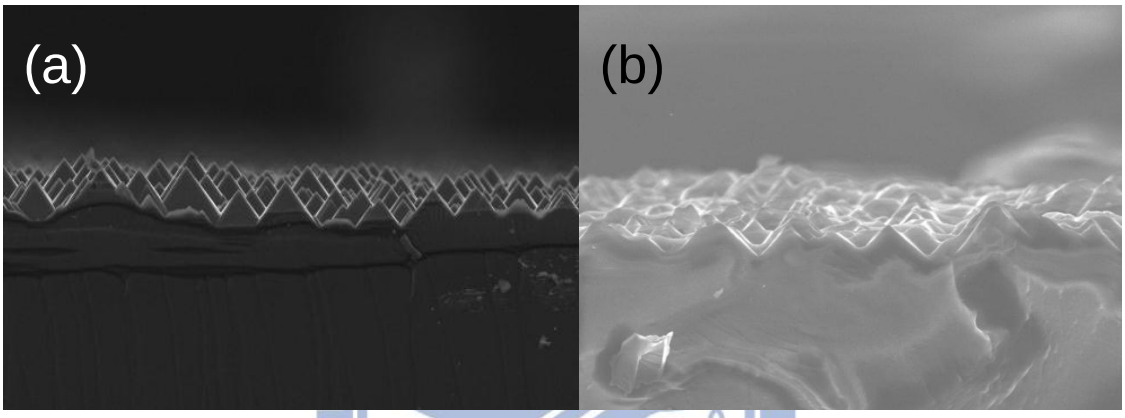

Figure 4.2.1-2 The textured substrate is prepared as (a). And the textured pattern is transformed by PDMS film as (b).

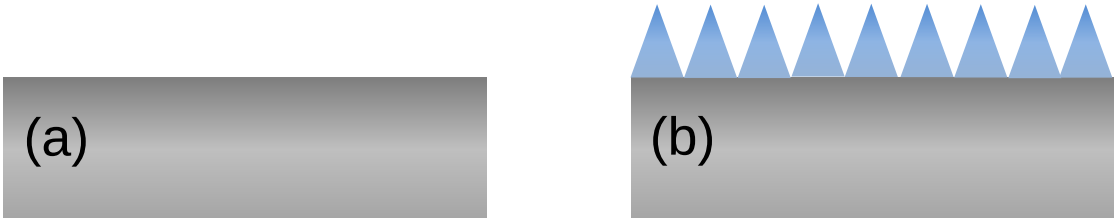

Figure 4.2.1-3 The cell was shown in (a). And the textured PDMS film was put on cell as (b).

4.2.2 The optical properties analysis of PDMS film

We measure the optics properties of flat PDMS and textured PDMS. From the results, the transmittance of both the flat and textured ones are very high(Figure 4.2.2-1). So it won't loss much energy. After that, we measure the Haze of both ones(Figure 4.2.2-2) , and the definition formula is below(4-1). It means the ratio with transmittance of scattering light by the total transmittance. From the figure, the haze of flat one is almost 0%, it means the light go out from the flat PDMS in straight. Otherwise, the Haze of textured one is very high, it means the light will scatter after go through the texture PDMS. And the optical path length is getting longer, which is benefit for solar cell to absorb more light.

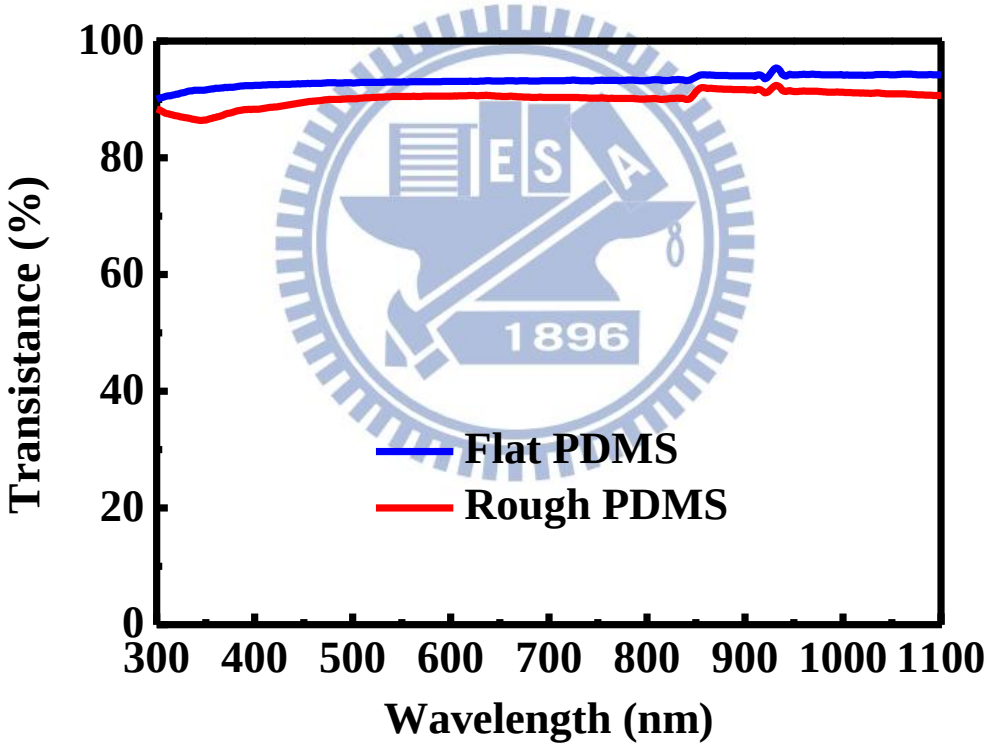

Figure 4.2.2-1 The transmittance of flat PDMS and rough PDMS.

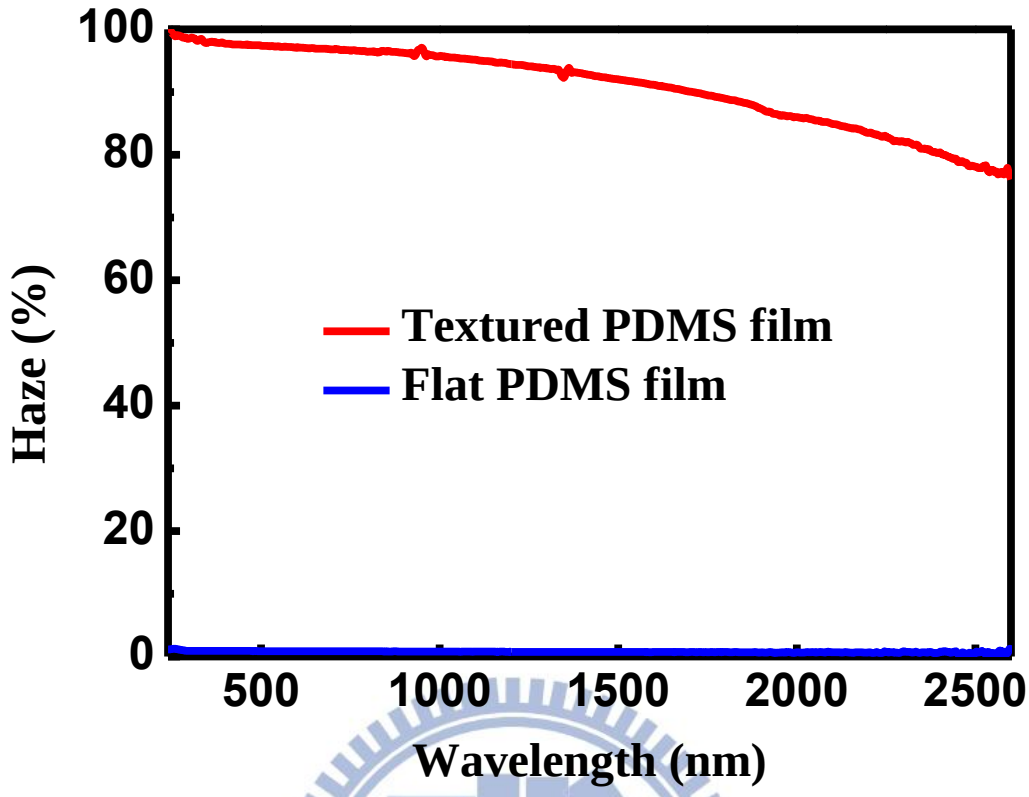

Figure 4.2.2-2 The haze of flat PDMS and rough PDMS.

$$Haze(\%) = \frac{T_{diff}}{T_{total}} \quad (4\text{-}1)$$

In order to understand how the scattering light capability of the flexible textured and flat PDMS films, we first measured the angle-dependent intensity of transmittance by bidirectional transmittance distribution function (BTDF) system with an incident light of 380 nm and ultraviolet-visible spectrophotometer. The system setup is shown in below(Figure 4.2.2-3). The light will go through the sample and scatter. And there is a detector moving as a circle to receive the light. So we will know the intensity of the scattered light with the angle. The results is shown in figure 4.2.2-4. The view angle of the flexible textured PDMS film at the full-width at half-maximum was enlarged from 12° to 48° compared with the flat PDMS film, which could be attributed to the increased light scattering by the textured structure as shown in Fig. 4.2.2-4. As the results, the introduction of the flexible textured PDMS film can

deflect the photons in much wider angle and lengthen the traveling distance in the cell, which implies higher possibility of getting absorbed.

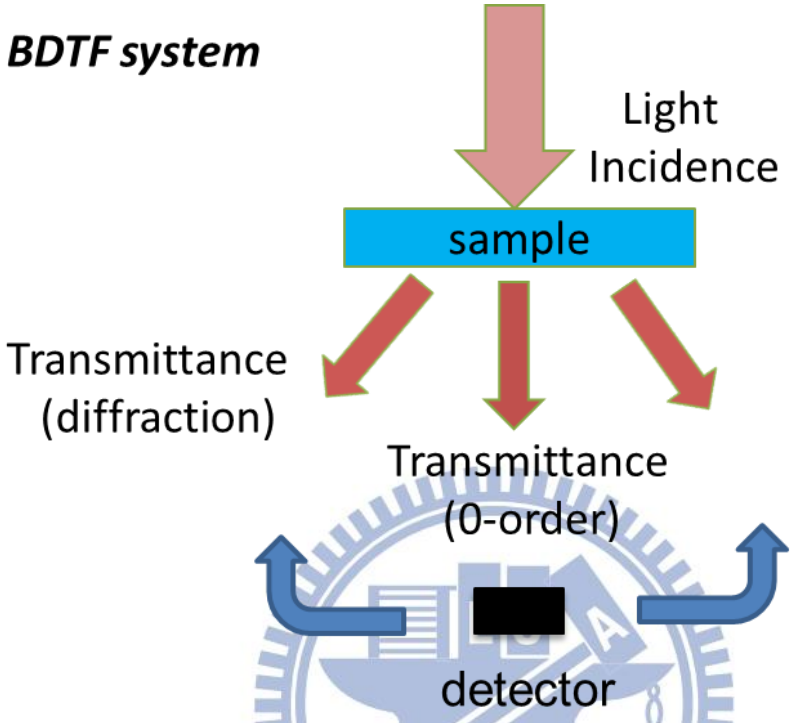

Figure 4.2.2-3 The chart of the bidirectional transmittance distribution function(BTDF) system

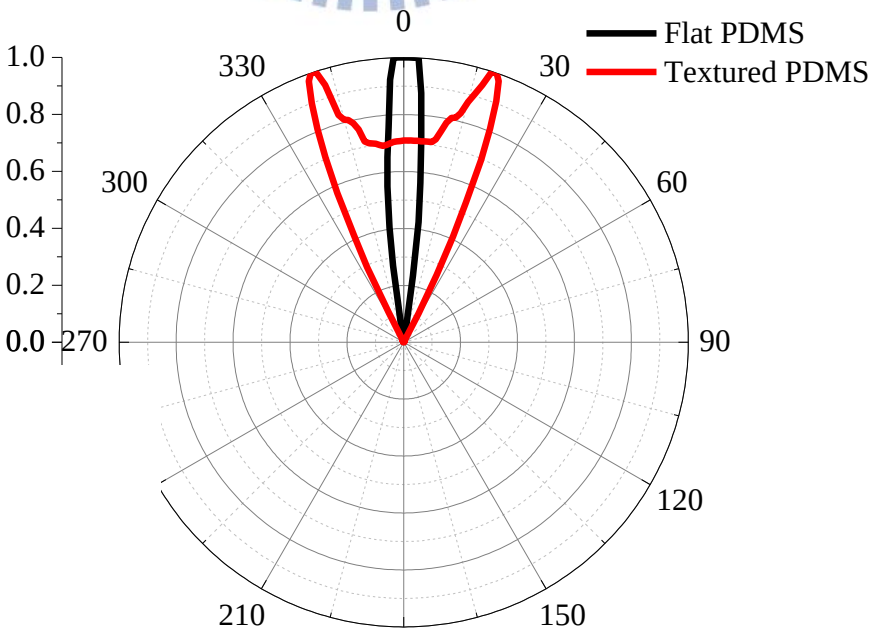

Figure 4.2.2-4 The intensity and the corresponding angle of flat and rough PDMS.

4.2.3 Reflectance spectrum

In order to confirm the broadband anti-reflectively characteristics of cell with PDMS, we measure the reflectance of reference cell, cell with flat PDMS and cell with rough PDMS by integrating sphere reflectance measurements, the lower reflectivity means the more light was absorbed with both flat and rough PDMS, the rough PDMS is better than flat PDMS because of the better anti-reflectively effect from graded refraction index effect.

Figure 4.2.3-1 shows the result of the measured reflectance of the reference cell, cell with flat PDMS and cell with rough PDMS under the light at normal incident. The result indicates the anti-reflective characteristic of cells with both flat and rough PDMS are better than reference cell over a broadband wavelength range. Especially at the wavelength of 350nm to 420nm which just mapping to the highest absorption range of GaN/InGaN multiple quantum well solar cell. For the cell with rough PDMS, we consider the reflectance is lower than cell with flat PDMS is caused by the scattering of the light, which enhance the optical path length. Otherwise, we consider the low reflectance was caused not only by anti-reflection characteristic but also by the light scattering characteristic of rough PDMS which can enhance the optical path length of long wavelength to further reduce the reflectance. The result indicates cell with PDMS has nice anti-reflective and enhance the light absorption and photo collection just confirm the idea we had before.

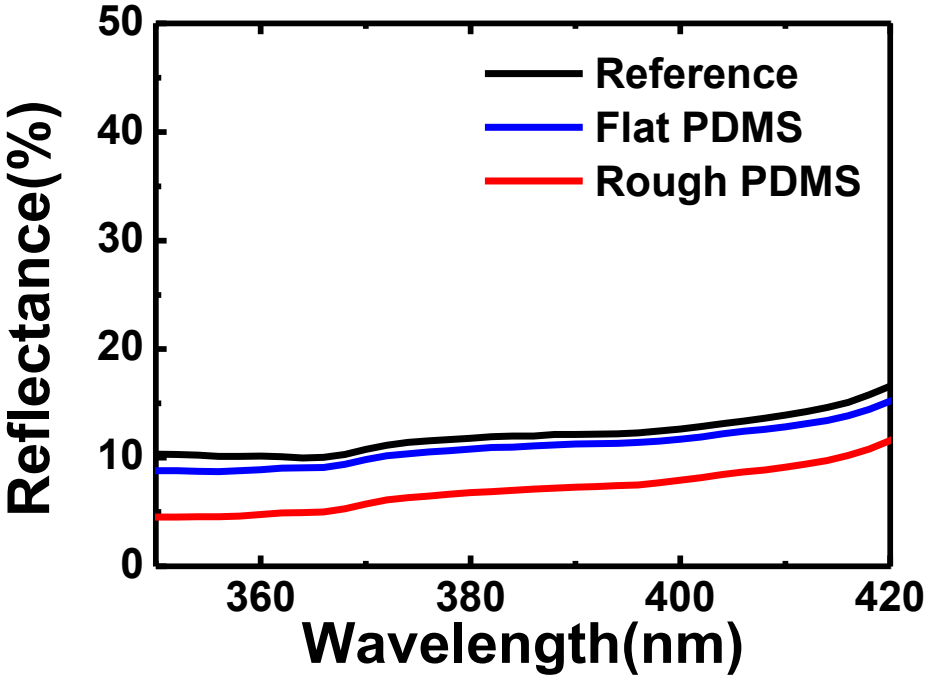

Figure 4.2.3-1 The measured reflectance of the reference cell, cell with flat PDMS and cell with rough PDMS.

4.2.4 Angular reflectivity

The incident-angle-dependent reflection properties are important to solar cells due to the sun movement. Here, we employ an angle-resolved reflectance spectroscopy to characterize the reference cell, cell with flat PDMS and cell with textured PDMS. The spectrum for the reference cell, cell with flat PDMS and cell with rough PDMS are shown in table 4.2-1.

The cold and warm colors in the color bar represent the low and high reflectance, respectively. Except for the reference cell, the reflectance of the both cell with flat PDMS and textured PDMS remains low at normal incidence and small angle of incidence(AOIs); however that of the reference cell gradually rise up at large AOIs. Compared to the cell with flat PDMS, the cell with rough PDMS shows the low optical reflection (R<10%) over the entire spectrum especially in the wavelength region which just mapping to the highest absorption range of GaN/InGaN multiple quantum well solar cell and an AOI up to 40°.

We demonstrate the cell with both flat PDMS and rough PDMS not only inhibit the broadband reflectivity at normal incidence but also reduce optical reflection at large incidence angle of light, promising a superior photocurrent generation over an entire day.

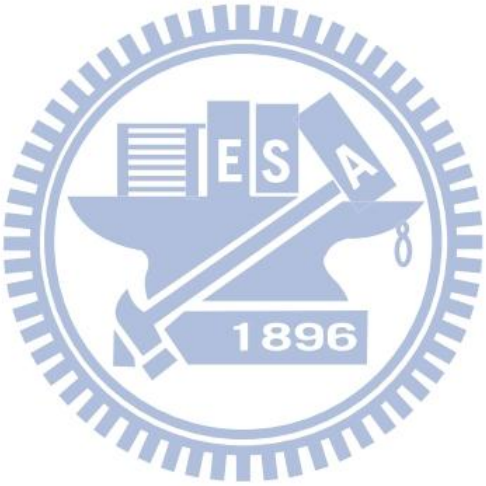

Reference cell
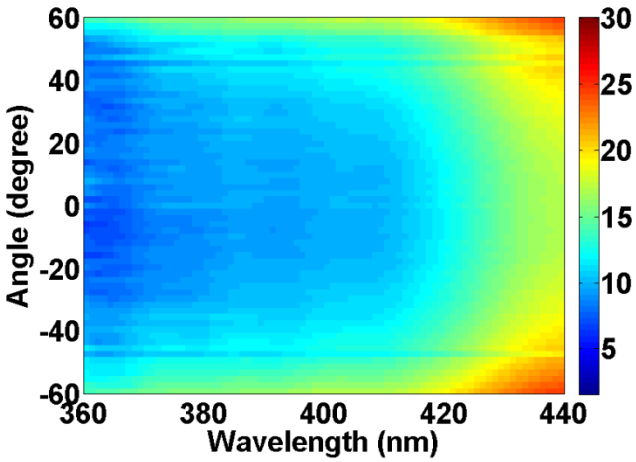
Cell with flat PDMS
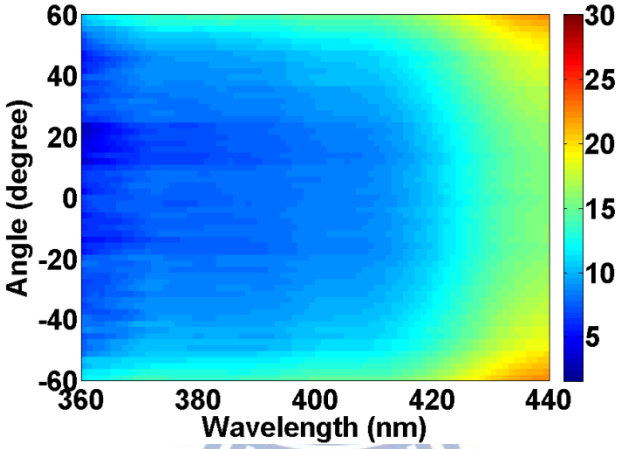
Cell with rough PDMS
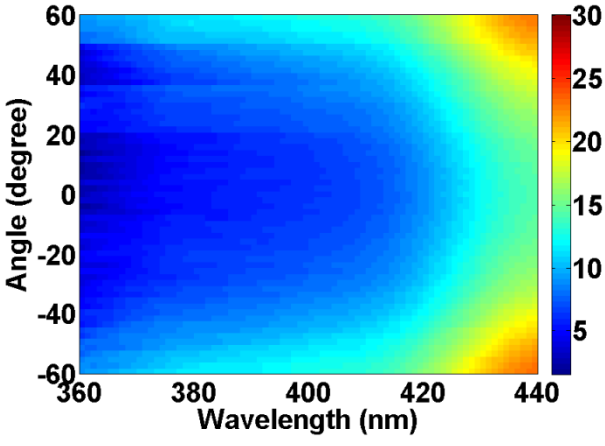

Table 4.2-1 The measured angular reflectance spectra for the reference cell, cell with flat PDMS and cell with rough PDMS.

4.2.5 The current-voltage (I–V) characteristics

In this study, the solar cell power conversion efficiency measurement system which includes, 1000W ClassA AM 1 .5 G solar spectrum which made by Newport company and calibrated with Renewable Energy Laboratory (NREL) and there is only 2% of error at each wavelength in international standards solar spectrum, then corrected incident sun light power intensity of 1 sun and maintain the temperature for the 25 ° C through the temperature control system, and then measure the current - voltage characteristics by Keithley 2400 source meter.

The current density-voltage curve of GaN solar cell, GaN soalr cell with flat PDMS, GaN soalr cell with rough PDMS are shown in Figure 4.2.5-1. The details of measured current-voltage characteristics are shown in table 4.2-2.

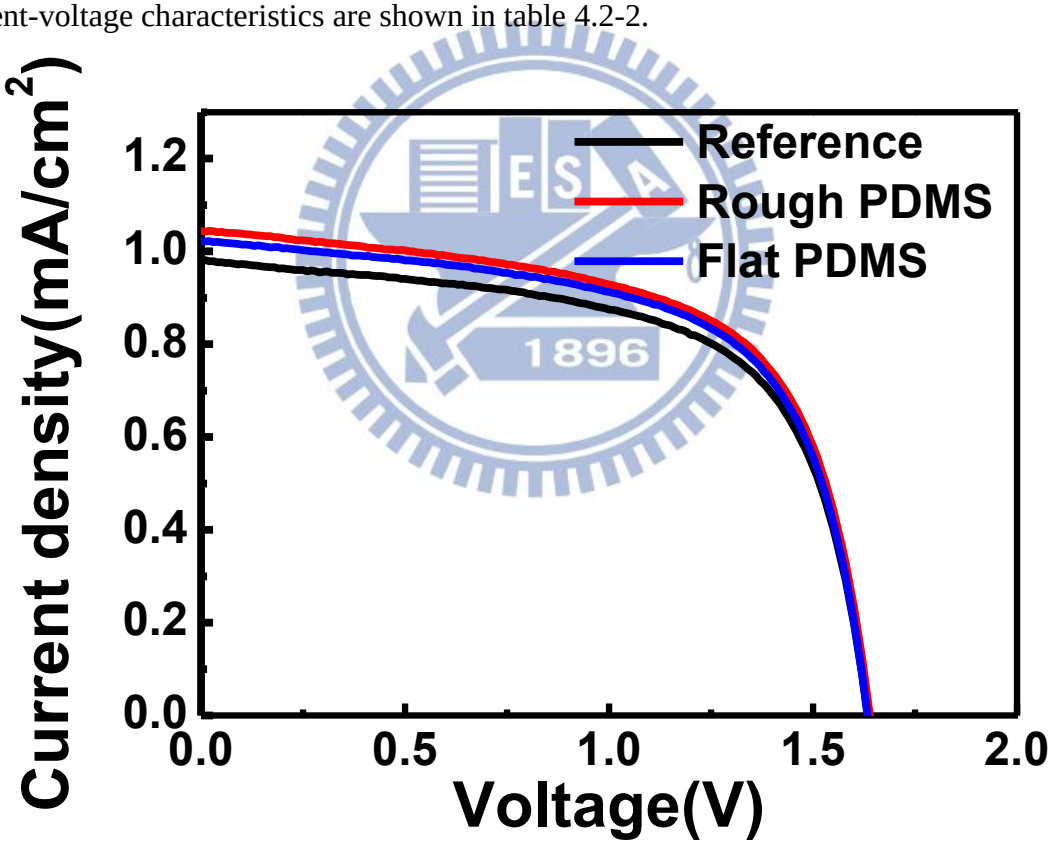

Figure 4.2.5-1 The measured current-voltage characteristics of Reference cell, cell with flat PDMS and cell with rough PDMS.

	Voc (V)	Jsc(mA/cm^2)	F.F.	Efficiency(%)
Reference	**1.63**	**0.98**	**62.78**	**1.001**
Flat PDMS	**1.63**	**1.02**	**62.87**	**1.049**
Rough PDMS	**1.64**	**1.05**	**62.63**	**1.072**

Table 4.2-2 The details of measured current-voltage characteristics of reference cell, cell with flat PDMS and cell with rough PDMS.

From the J-V curve result, we can observe the J_{sc} of flat PDMS cell and rough PDMS cell is higher than the reference ones. It means the more photon is absorbed, and generates more electron-hole pairs. And more photons are absorbed because of the anti-reflection effect. We can prove PDMS is a newable material that can have the the effect of anti-reflection. And J_{sc} of rough PDMS solar cell is higher than flat ones is because of the effective medium theory mentioned before. Otherwise, there are structures on the top, it will scatter the light just as we measured before. So the enhancement is from the effect of light trapping, the light will go through a longer optical path length.

The GaN solar cell with flat PDMS layer can effectively enhance the short-circuit current density from 0.98 to 1.02 mA/cm^2 and the power conversion efficiency from 1.001 to 1.049 %, corresponding to a 4.8 % enhancement compared to one without textured PDMS of GaN solar cell.

The GaN solar cell with textured PDMS layer can effectively enhance the short-circuit current density from 0.98 to 1.05 mA/cm^2 and the power conversion efficiency from 1.001 to 1.072 %, corresponding to a 7.1 % enhancement compared to one without textured PDMS of GaN solar cell.

The open-circuit voltage (V_{oc}) and the fill-factor (FF) in GaN solar cell exhibit negligible change, because the textured PDMS film was pasted up on the surface of GaN solar

cell and did not interfere with the diode operation.

4.2.6 External quantum efficiency (EQE)

To understand more thoroughly on the interaction of the textured PDMS with photons into the GaAs solar cell, we measured the spectral response of the external quantum efficiency (EQE). Figure 4.2.6-1 shows the external quantum efficiency (EQE) as function of illumination wavelength for all three types of solar cells (with textured PDMS, with flat PDMS, and without any coating).

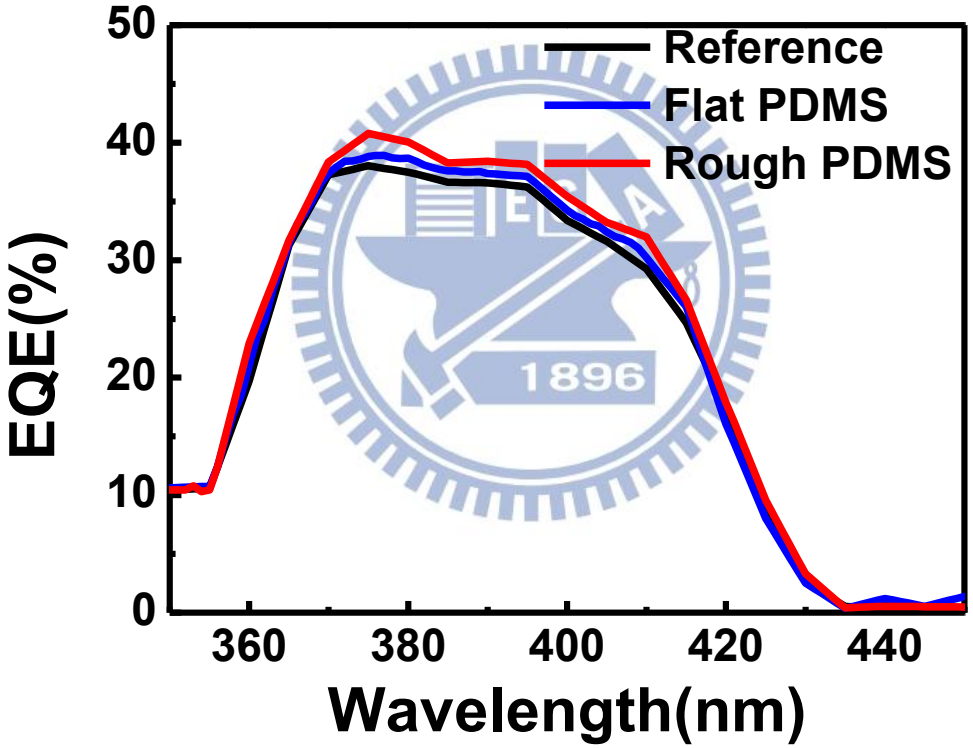

Figure 4.2.6-1 The measured external quantum efficiency of reference cell, cell with flat PDMS and cell with rough PDMS.

The EQE of GaN solar cell with both flat and rough PDMS show a significantly EQE enhancement in broadband, from the wavelength 350nm to 440nm, just matching the best absorption region of GaN solar cell. And the EQE enhancement is resulted from antireflection

effect.

The GaN solar cell with textured PDMS film can offer a superior anti-reflective property in the range of wavelength from 350 nm to 440 nm, compared with the cell without textured PDMS film, and this result agrees with measurement of EQE. The reduction of reflectance means more photons can get into the devices due to suitable refractive index of textured PDMS film (n~1.42) and the increase of light scattering due to the introduction of the textured PDMS; hence, more carriers can be generated, and an increase of photocurrent accordingly. From these experiments, we could found the textured PDMS film on GaN solar cell surface brings several advantages: first is the reduction of reflectance; second is the increase of light scattering at the surface; third is a simple fabrication process. All these effects can greatly improve the short-circuit current density with our conventional GaN-based solar cells.

4.2.7 Nano scale PDMS film

One advantage of PDMS is its transformation ability. And the PDMS is flexible for different kinds of substrate. Here we made the nano-scale PDMS film. We all know if we make the right ratio of the diameter to the wavelength of the incident light. We can make the reflectance very low. In this way, the nano-scale PDMS film is a very important concept. Figure 4.2.7-1 shows the SEM images of the the textured nano-scale substrate(figure 4.2.7-1(a)) and the nano-scale PDMS film was successfully achieved from the method mentioned before(figure 4.2.7-1(b))

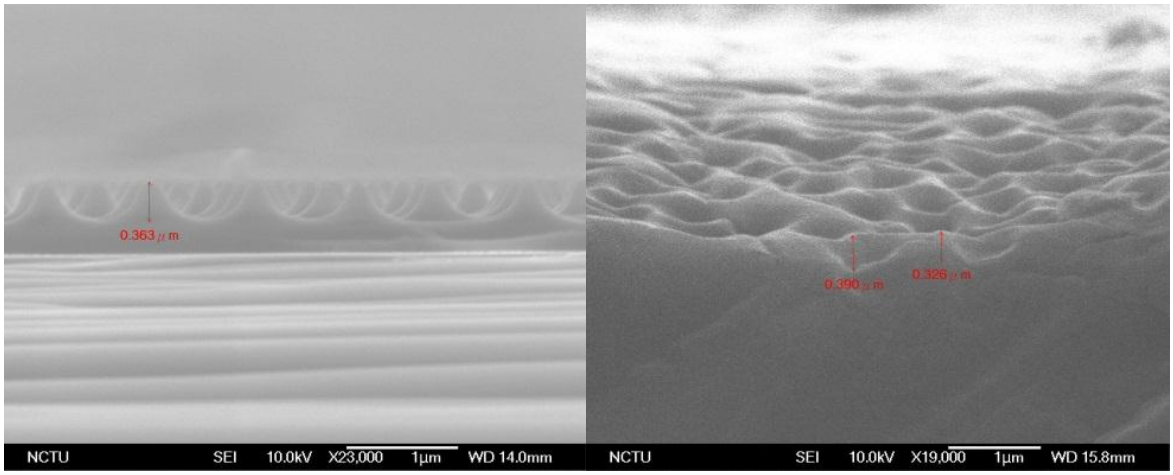

Figure 4.2.7-1 The SEM images of the nano-scale textured substrate(a); and the transformed nano-scale PDMS film(b).

From the J-V curve result(figure 4.2.7-2), we can observe the J_{sc} of nano-scale PDMS cells higher than the reference ones. It means the more photon is absorbed, and generates more electron-hole pairs. And more photons are absorbed because of the anti-reflection effect. The details of measured current-voltage characteristics are shown in table 4.2-3.

The GaN solar cell with nano-scale PDMS layer can effectively enhance the short-circuit current density from 0.98 mA/cm^2 to 1.03 mA/cm^2 and the power conversion efficiency from 1.001 to 1.051 %, corresponding to a 5 % enhancement compared to one without textured PDMS of GaN solar cell.

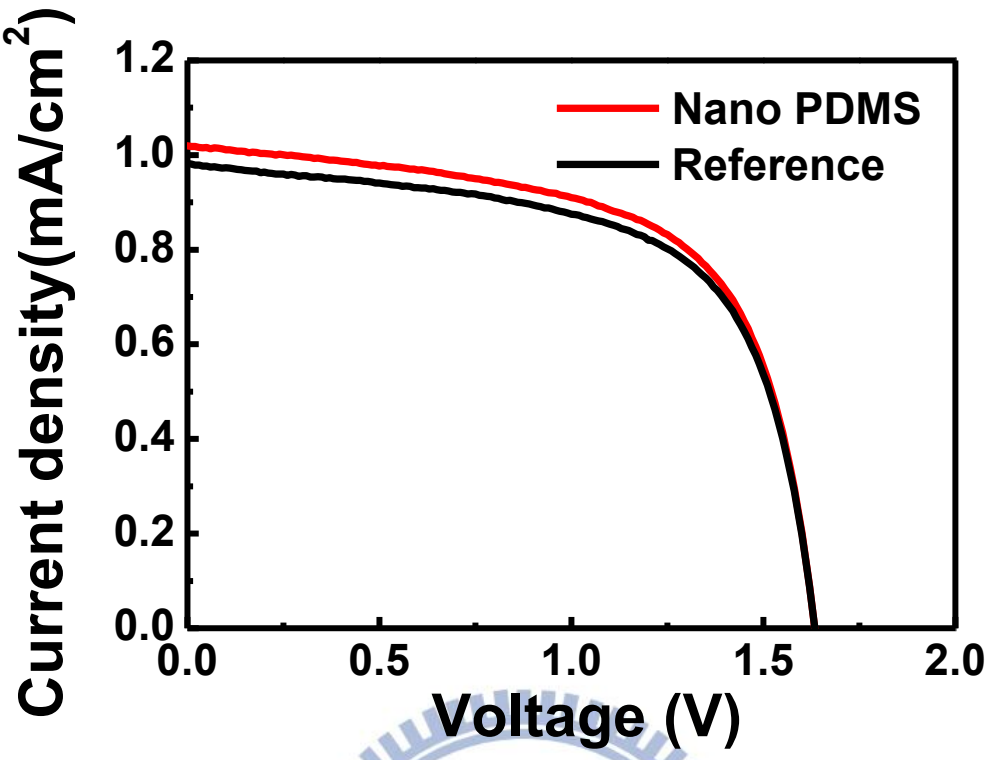

Figure 4.2.7-2 The measured current-voltage characteristics of Reference cell and cell with nano-scale rough PDMS.

	Voc (V)	Jsc(mA/cm^2)	F.F.	Efficiency(%)
Reference	**1.63**	**0.98**	**62.78**	**1.001**
Nano PDMS	**1.63**	**1.03**	**62.88**	**1.051**

Table 4.2-3 The details of measured current-voltage characteristics of reference cell and cell with nano-sclae rough PDMS.

The EQE of GaN solar cell with nano-scale rough PDMS show a significantly EQE enhancement in broadband compared to reference ones(figure 4.2.7-3), from the wavelength 350nm to 440nm, just matching the best absorption region of GaN solar cell. And the EQE

enhancement is resulted from antireflection effect.

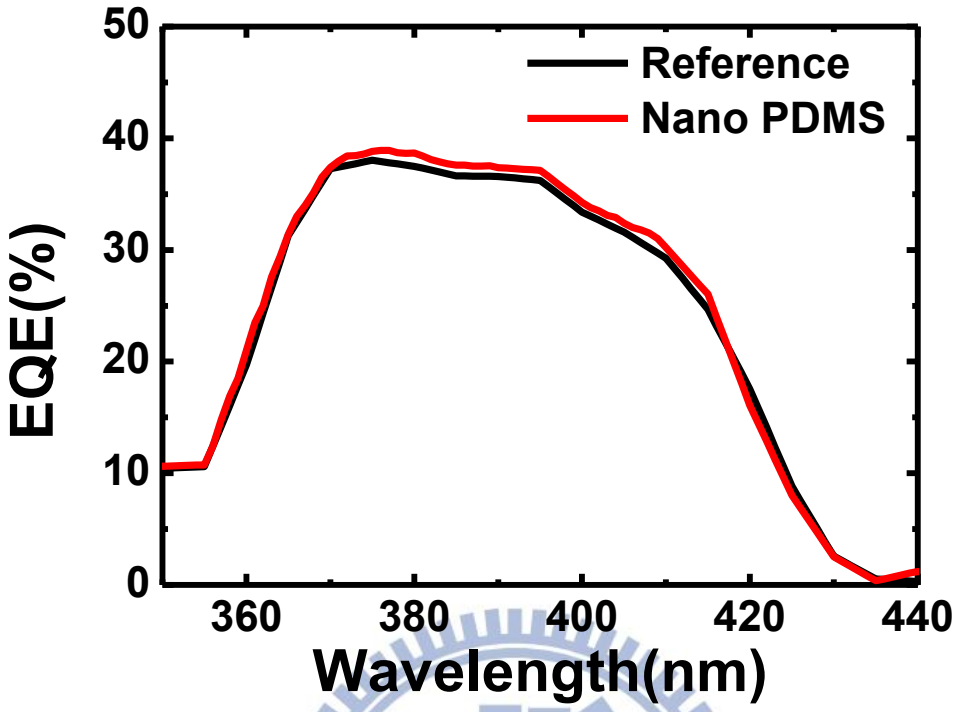

Figure 4.2.7-3 The measured external quantum efficiency of reference cell and cell with nano-scale rough PDMS.

We successfully make out the nano-scale PDMS, and put on the GaN-bsaed cell to get the higher efficiency. I believe it will be a popular material used on solar cell in some days because it have so many advantages such as low-cost, non-vacuum system and simple process and large area, and the PDMS film is flexible, it can use in many substrate. The most important point is it don't make the electricity property poor. That's why it's a successful novel materials.

4.3 Quantum dots (QDs)

Quantum dots (QDs) is a new material apply for solar cells. The benefits of adapting quantum dot material in the solar cell are mainly for low-cost, large area, flexible substrates potentially high efficiency and photon down conversion center. One of the major limits in current solar cell is the lack of absorbing material at ultraviolet (UV) region. These high energy photons get absorbed quickly in the bulk material but the carriers are consumed near the surface by the traps and defects. This portion of sunlight takes up to 7% of the overall energy [37], and this percentage is even higher in the outer space. Therefore, efficient use of UV part of the solar spectrum for energy conversion is crucial. If UV photons can be harvested, it is then possible to enhance the efficiency.

Quantum dots (QDs) materials are a good down converter materials abundant in earth.[37] The reduced dimensionality of QDs exhibits quantization of their electronic energy levels, and consequently the blue-shift of optical absorption edge takes place. Because the QDs electronic energy levels and optical spectrum depend on their size, the effective band gap can be tuned for the solar spectrum.[38] In addition, due to the low cost and easy fabrication, casting the QDs films from colloidal methods has been explored for solar cells applications.[39]

The figure 4.3-1 shows the absorption and EQE of the GaN/InGaN solar cell, and we can see the poor collection of electron-hole pairs in the short wavelength region. So we measured the absorption of Front ITO layer(figure 4.3-2) and discover that the absorption of ITO material is very large in the short wavelength region, which cause the poor collection of carriers.

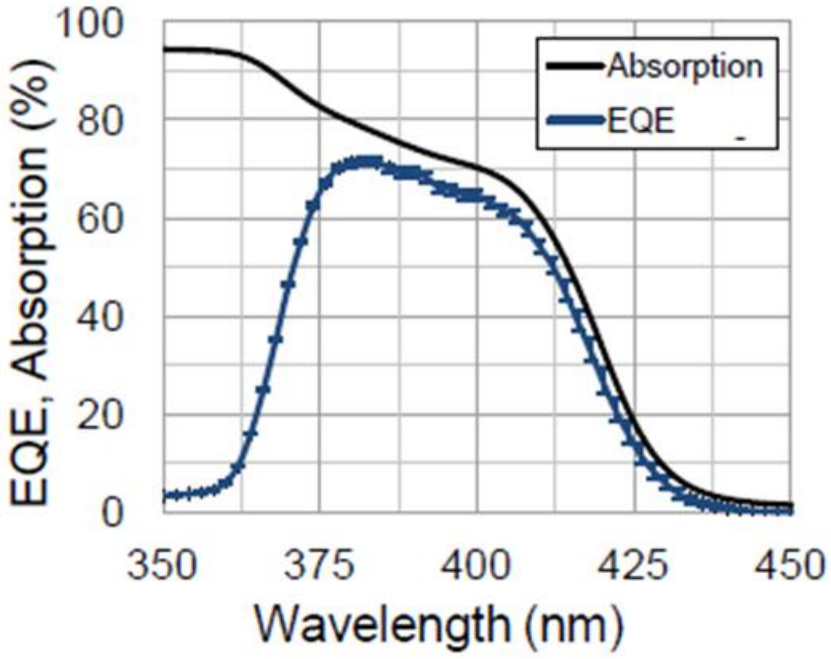

The figure 4.3-1 The absorption and EQE of the GaN/InGaN solar cell.[40]

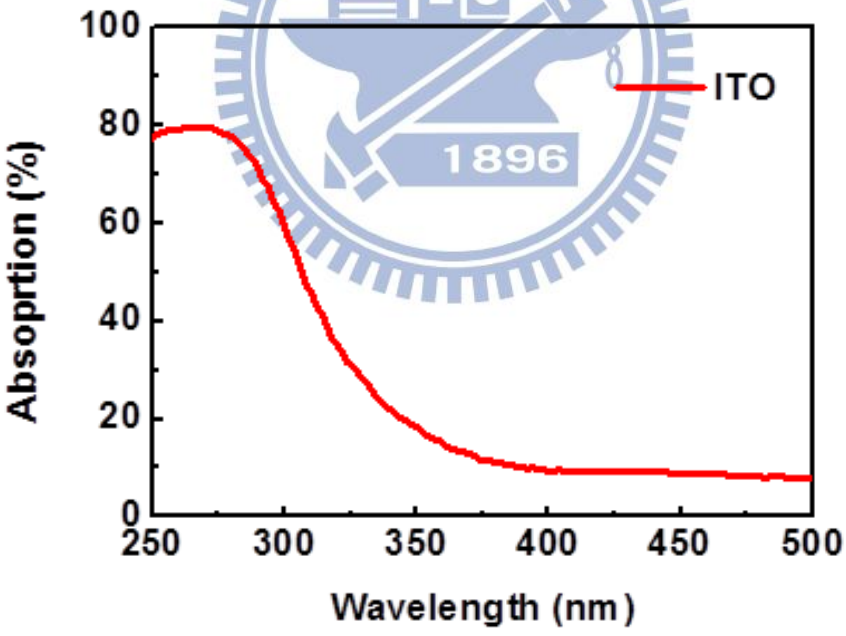

Figure 4.3-2 The absorption of Front ITO layer.

If we can use these UV region, we must can enhance the efficiency of GaN/InGaN solar cells. So quantum dot is the key technique to solve this problem. The figure 4.3-3 shows the absorbance and photoluminescence spectrums of CdS QDs in toluene. The photoluminescence spectrum was measured by the 365 nm excitation, and a major emission

peak at 460 nm was found. In absorbance spectrum, a sharp rising edge was detected around 450nm and a steady increase from 400 nm on. Therefore, this CdS QD layer is capable of converting ultraviolet photons (λ<400nm) to the visible blue band. So we can spread the quantum dots on the cells, it can absorb the UV region light before ITO layer and converting to visible region light that ITO can not absorb. In this way, we can solve the problem mentioned before, just by adding some CdS quantum dots material.

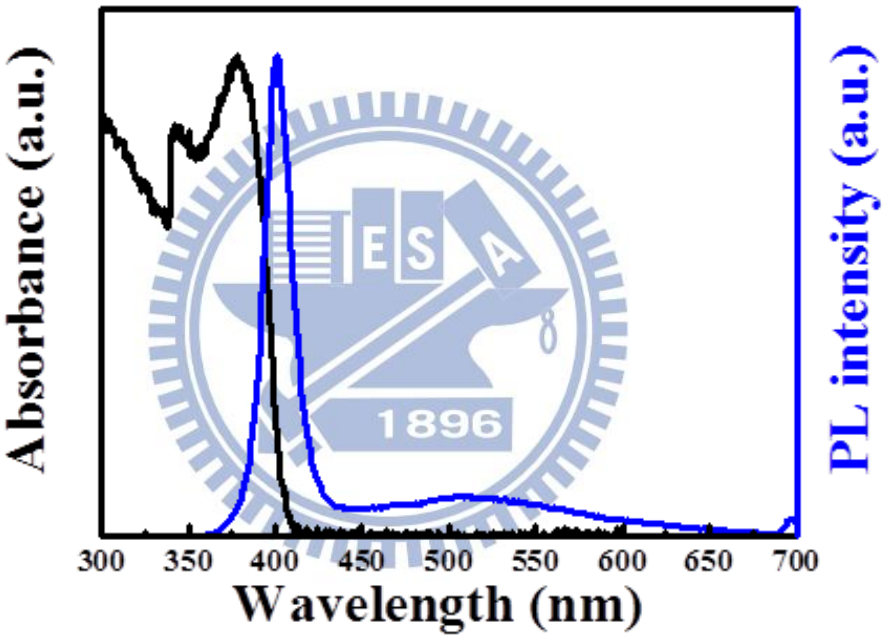

Figure 4.3-3 The absorbance and photoluminescence spectrums of CdS QDs in toluene.[41]

4.3.1 Reflectance property

So we spread the QDs on the cell to see if the efficiency is improved(figure4.3.1-1). Figure 4.3.1-2 shows the result of the measured reflectance of the reference cell and cell with QDs under the light at normal incident. The result indicates the anti-reflective characteristic of cells with QDs is better than reference cell over a broadband wavelength range. Especially at

the wavelength of 350nm to 420nm which just mapping to the highest absorption range of GaN/InGaN multiple quantum well solar cell. We prove that the cell with QDs has the anti-reflectance coating effect.

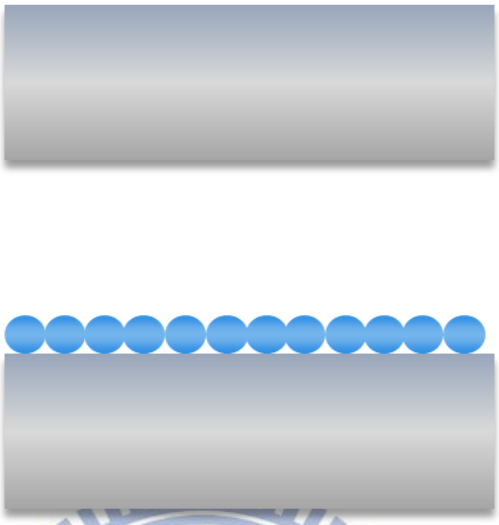

Figure 4.3.1-1 The chart of the reference cell and cell with QDs.

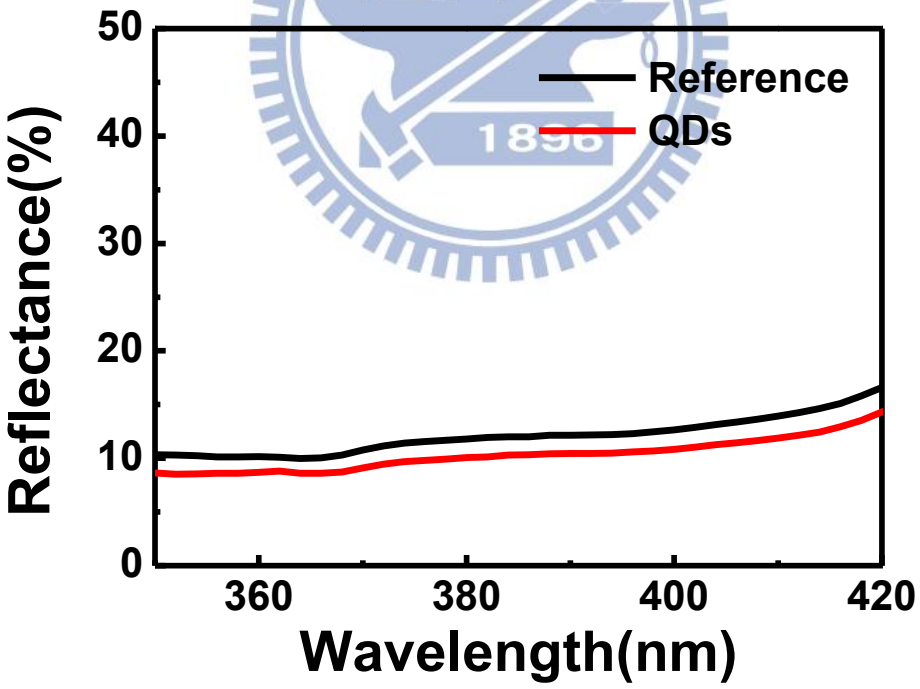

Figure 4.3.1-2 The measured reflectance of the reference cell and cell with QDs.

Otherwise, we measured the incident-angle-dependent reflection properties.(table 4.3-1) Except for the reference cell, the cell with QDs remains low at normal incidence and small angle of incidence(AOIs); however that of the reference cell gradually rise up at large AOIs.

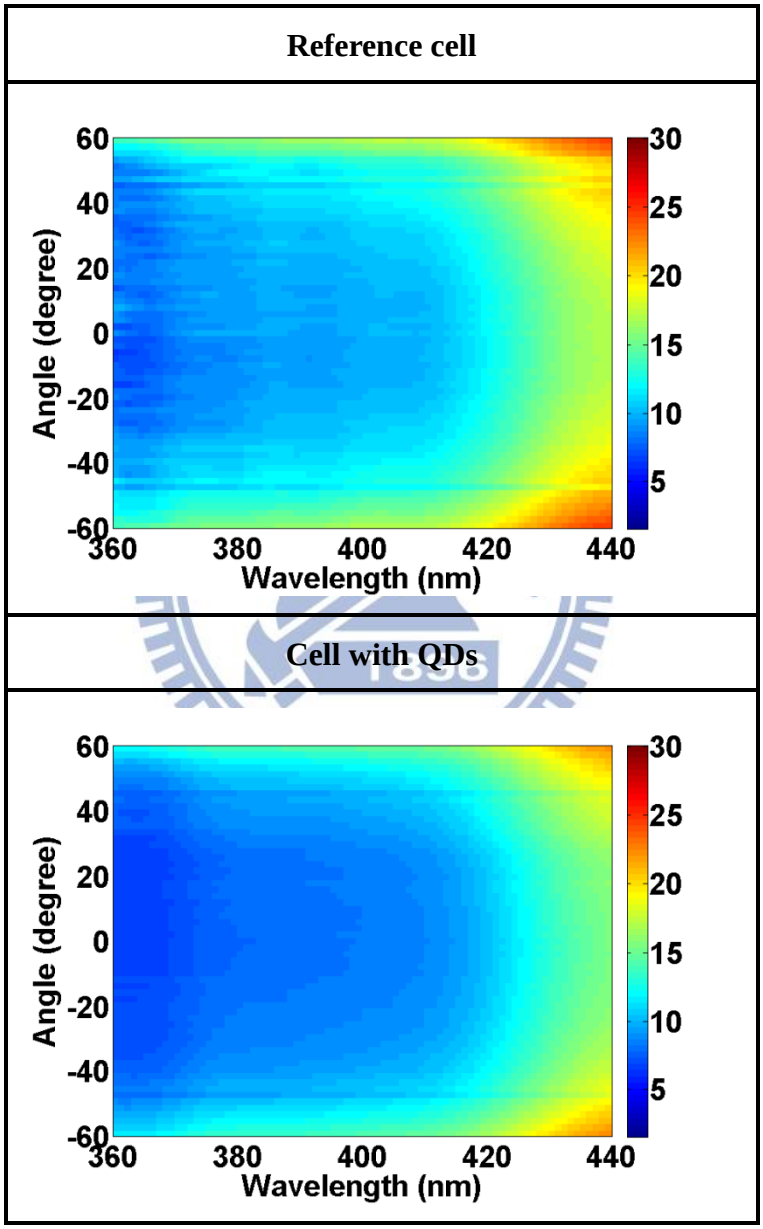

Table 4.3-1 The measured angular reflectance spectra for the reference cell and cell with QDs.

4.3.2 The current-voltage (I–V) characteristics

The photovoltaic I-V characteristic were measured under air mass 1.5 global illumination and room temperature conditions by a class-A solar simulator complying with the IEC 904-9 standard. The results was shown in Fig. 4.3.2-1. The device characteristics were summarized in Table 4.3-2.

The GaN solar cell with QDs layer can effectively enhance the short-circuit current density from 0.95 to 1.01 mA/cm^2 and the power conversion efficiency from 0.97 to 1.03 %, corresponding to a 7.2 % enhancement compared to reference ones.

From the J-V curve result, we can observe the J_{sc} of cell with QDs is higher than the reference ones. It means the more photon is absorbed, and generates more electron-hole pairs. And more photons are absorbed because of the QDs. It convert the light in UV region to visible region before ITO layer so the light in UV region doesn't loss.

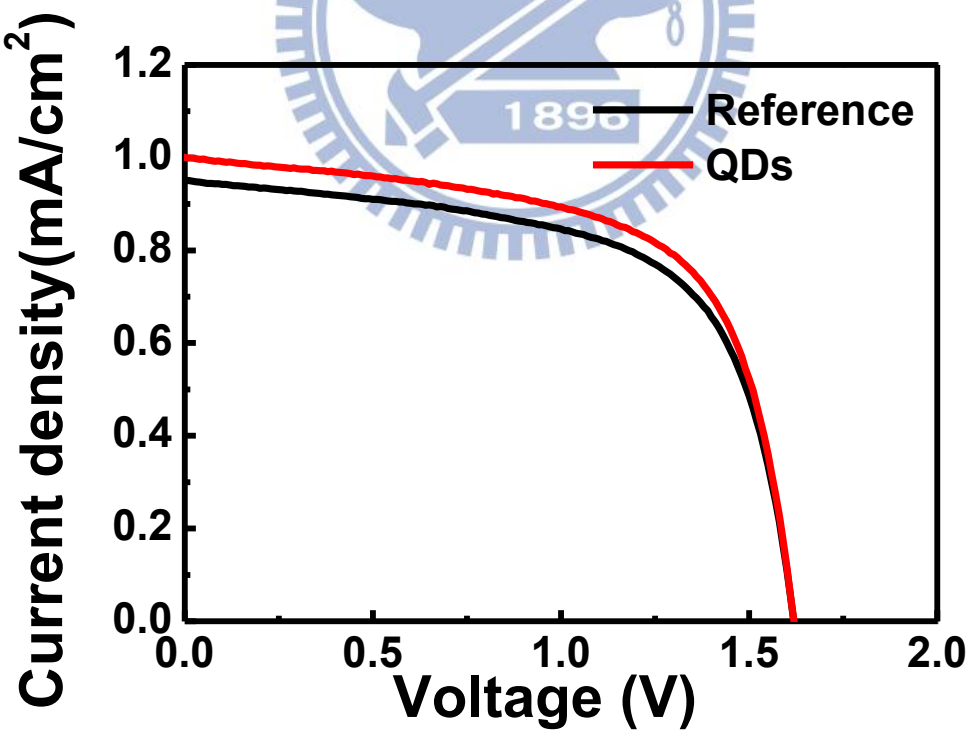

Figure 4.3.2-1 The measured current-voltage characteristics of Reference cell and cell with QDs.

	Voc (V)	Jsc(mA/cm^2)	F.F.	Efficiency(%)
Reference	**1.62**	**0.95**	**62.82**	**0.97**
400nm QDs	**1.62**	**1.01**	**63.42**	**1.03**

Table 4.3-2 The details of measured current-voltage characteristics of reference cell and cell with QDs.

4.3.3 External quantum efficiency

However, it is still unclear whether this improvement is from down-conversion photons or from other factors. To understand more thoroughly on the interaction of QDs with photons, we measured the spectral response of the external quantum efficiency (EQE).

Figure 4.3.3-1 shows the EQE of the reference cell and cell with CdS QDs layers. The cell with CdS QDs layers shows an enhanced EQE in the range from 350nm to 440nm. Especially in the range 350nm to 400nm, it shows the higher enhancement, just matching to the absorption of the QDs.

The overall shape of EQE enhancement resembles the absorption curves of QDs, and we believe this is a strong indication of QD absorption and down-conversion process. Most of electron–hole pairs generated in this UV regime are located near surface of device, and the surface defects consume most of the photo-generated carriers, which lead to inferior cell efficiency in UV wavelength range. Therefore, the addition of CdS QDs layers on the GaN solar cell can produce photon down-conversion effect, in which QD-originated photons with visible wavelengths can be absorbed in the depletion region, and the power conversion efficiency is improved. On the other hand, when the incident photons' wavelength is longer than 400nm, the QDs layer is served more like an AR coating, which can also enhance the light harvesting.

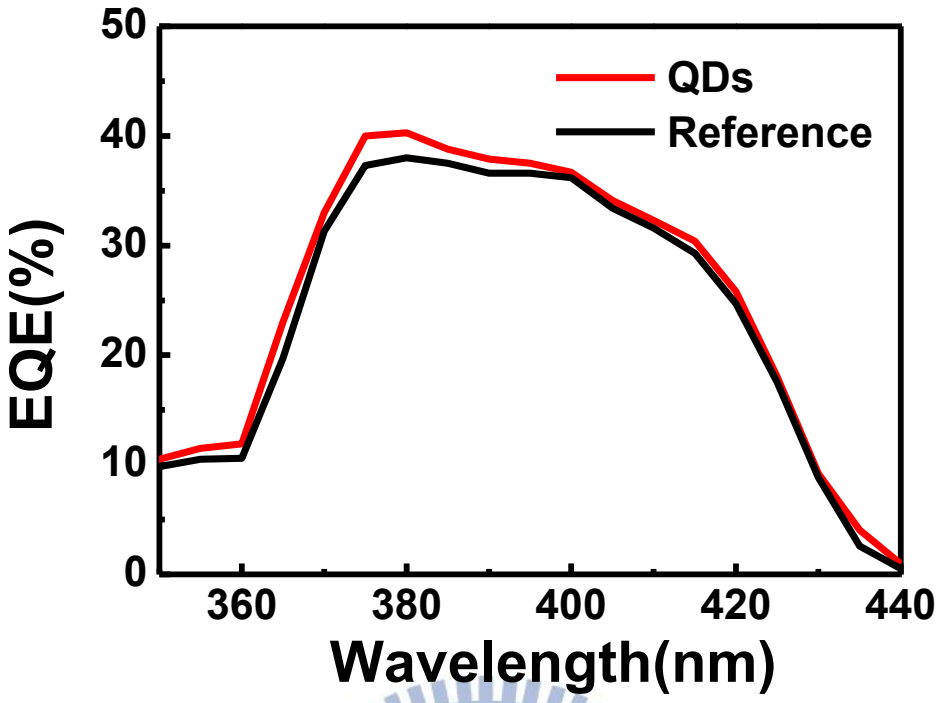

Figure 4.3.3-1 The measured external quantum efficiency of reference cell and cell with QDs.

4.3.4 DBR effect

After then, we measured the transmittance of the cell with QDs. And we found out the transmittance of the cell with QDs is still high(figure 4.3.4-1). That means many photons loss, we didn't get use of it. So we think how to solve this situation, and comes the DBR material in.

From figure 4.3.4-1, we observe the transmittance of cell with QDs is slightly higher than reference. The reason is the anti-reflectivity characteristic of QDs. QDs let more light in the cell, but it can't absorb all of them. So some light come out the cell.

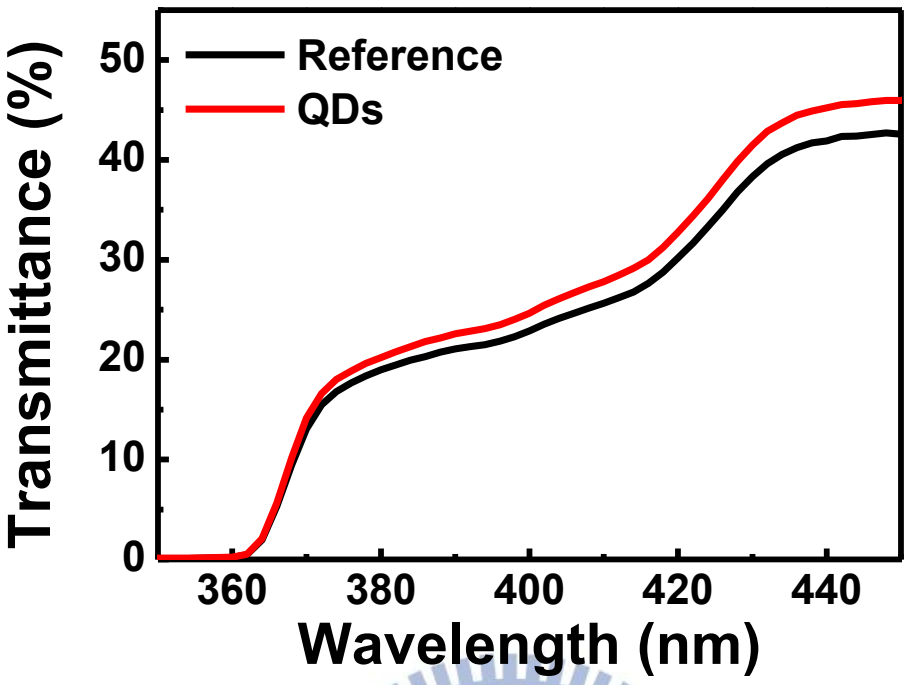

Figure 4.3.4-1 The measured transmittance of reference cell and cell with QDs.

DBR can reflect the light of specific wavelength. We design a DBR that reflect the light effectively from 370nm to 430 nm. The reflectance spectrum is shown in figure 4.3.4-2.

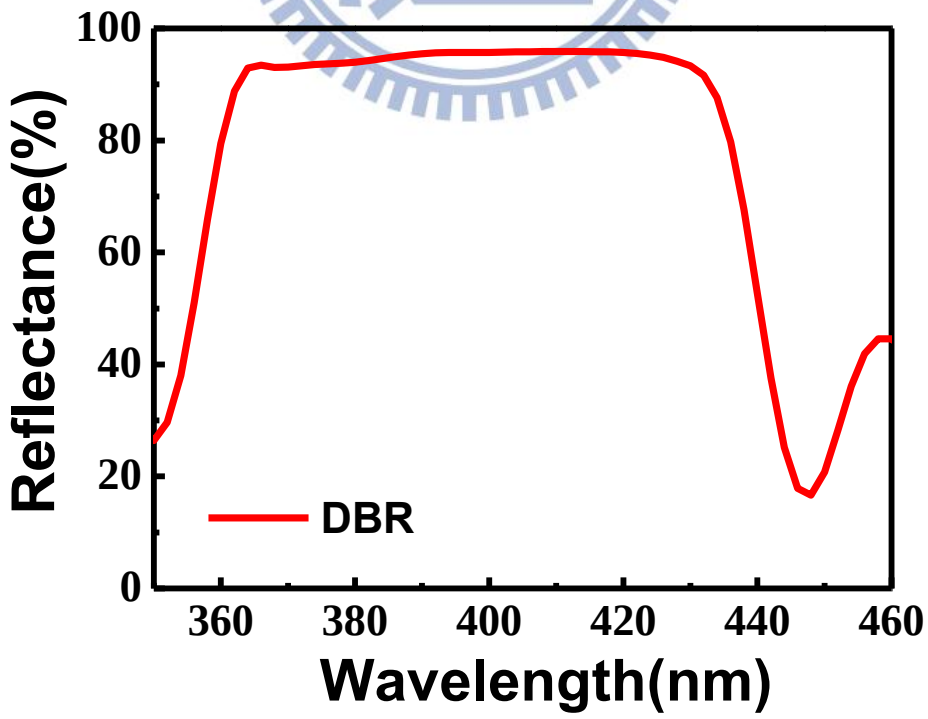

Figure 4.3.4-2 The measured reflectance of DBR.

From figure 4.3.4-2, we observe the reflectance of DBR is very high (R>95%). We think that may reduce the problem mentioned before. So we add the DBR to the back of the cell and want to reflect the light into cell to be used again. We measured the absorption spectrum of reference cell, cell with QDs, cell with DBR and cell with both QDS and DBR(figure4.3.4-3).

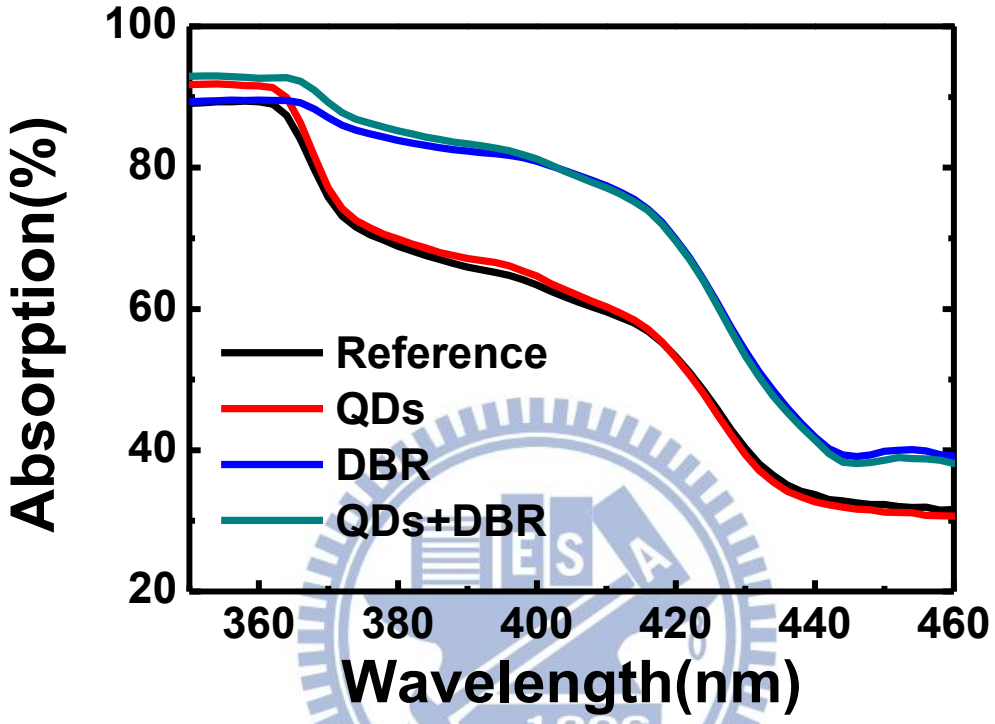

Figure 4.3.4-3The absorption spectrum of reference, cell with QDs, cell with DBR and cell with both QDS and DBR.

We can see the cell with QDs is higher than reference before 400nm, it means the QDs do convert the light into the cell to be used. And the cell with DBR is higher after 370nm because it reflect the light back to the cell to be used again. As we expect, the best absorption is the cell with QDs and DBR. It shows the broadband enhancement in absorption from 350nm to 460nm.

So we measured the J-V curve to see if the efficiency is improved. The results is shown in figure 4.3.4-4. We compare the reference cell, cell with QDs and cell with both QDs and DBR. The device characteristics were summarized in Table 4.3-3.

The cell with both QDs and DBR can effectively enhance the short-circuit current density from 1.01 to 1.15 mA/cm^2 and the power conversion efficiency from 1.019 to 1.162 %,

corresponding to a 14 % enhancement compared to cell with QDs.

From the J-V curve result, we can observe the J_{sc} of cell with DBR is higher than the reference ones and cell with QDs. It means the more photon is absorbed, and generates more electron-hole pairs. And more photons are absorbed because of the reflection of the DBR. It reflect the light into the cell to be use again, and reduce the loss in photon.

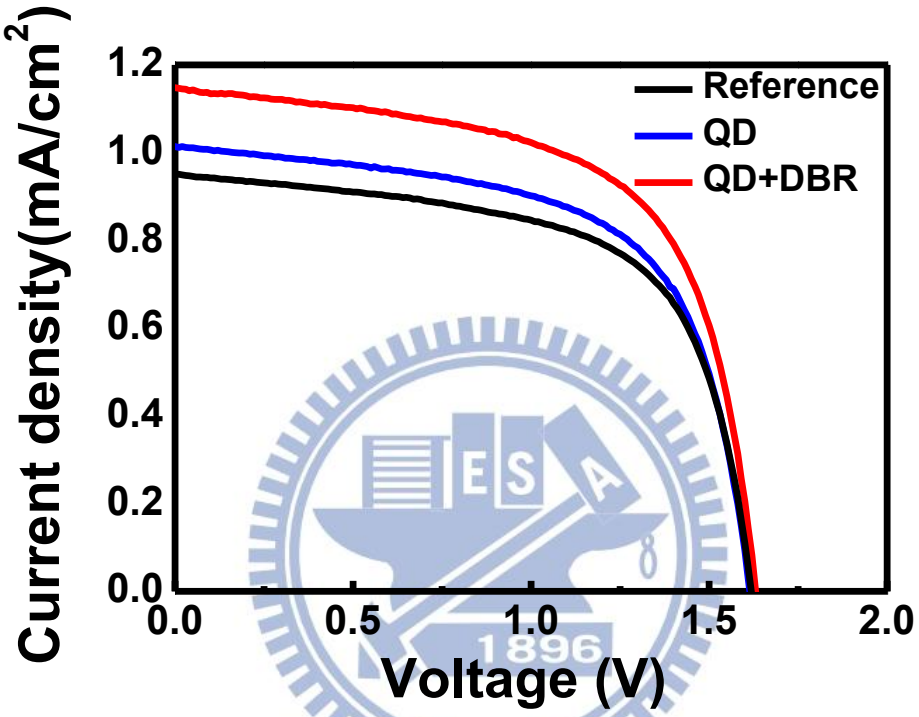

Figure 4.3.4-4 The measured current-voltage characteristics of reference cell, cell with QDs and cell with both QDs and DBR.

.

	Voc (V)	Jsc(mA/cm2)	F.F.	Efficiency(%)
Reference	**1.62**	**0.95**	**62.82**	**0.97**
QDs	**1.61**	**1.01**	**62.28**	**1.019**
QDs+DBR	**1.63**	**1.15**	**62.23**	**1.162**

Table 4.3-3 The details of measured current-voltage characteristics of reference cell, cell with QDs and cell with both QDs and DBR

After all, we measured the external quantum efficiency of the reference, cell with QDs

and cell with QDs and DBR.

Figure 4.3.4-5 shows the EQE of the reference cell, cell with QDs and cell with QDs and DBR. The cell with DBR and QDs layers shows an enhanced EQE in the range from 350nm to 440nm. Especially in the range 350nm to 420nm, it shows the higher enhancement, just matching to the high reflectance of the DBR.

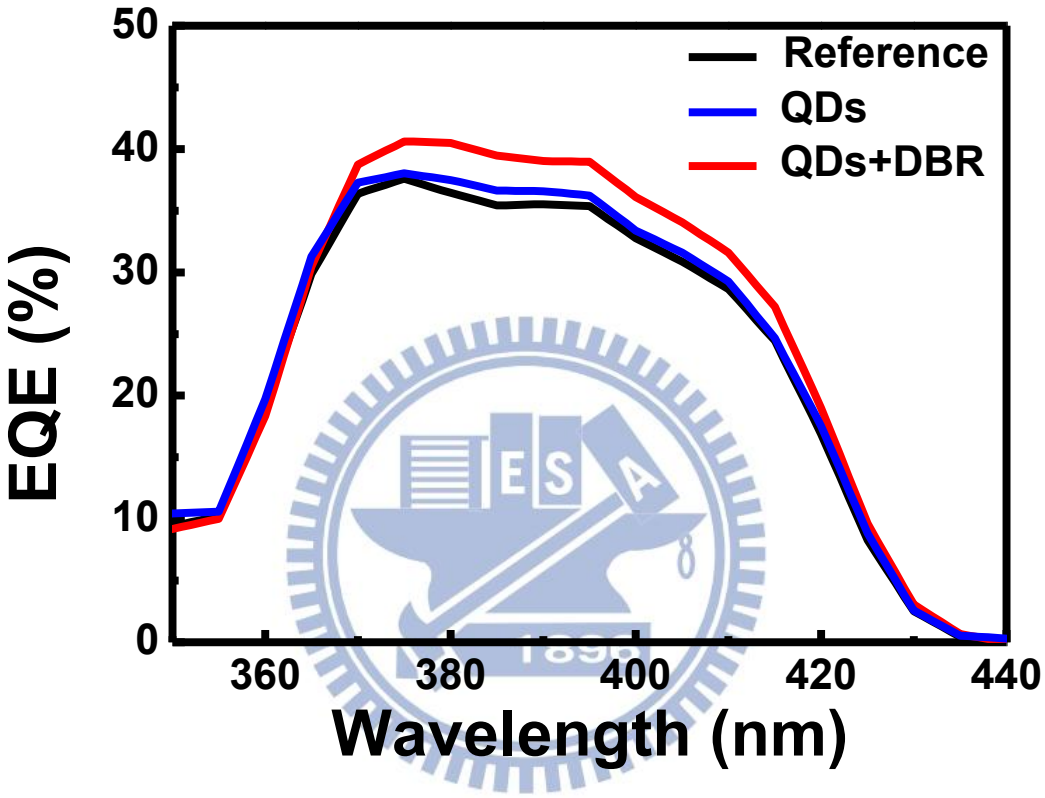

Figure 4.3.4-5 The measured external quantum efficiency of reference cell, cell with QDs and cell with both DBR and QDs.

Chaper 5. Conclusion

In summary, we successfully demonstrate the textured PDMS film serve as anti-reflectance coating layer. The advantages are the low-cost, non-vacuum system, large area and simple process. PDMS film provides a refractive index gradient to reduce the reflectance. From the reflectance spectroscopy and angle-resolved reflective spectra, we observe that both flat and rough PDMS show the the better omnidirectional and broadband anti-reflective characteristic (ARC) compared to reference cell.

Then we demonstrated the PDMS film which is useful in harvesting solar photon and enhancing the power conversion efficiency of InGaN/GaN multiple quantum well solar cells. Compared cell with flat PDMS and cell with rough PDMS to reference one, the power conversion efficiency achieved 4.8% and 7.1% enhancement, and the J_{sc} achieved 4.1% and 7.2% enhancement respectively.

Second part, we successfully demonstrate the quantum dots(QDs) serve as photon down conversion centers. From the reflectance spectroscopy and angle-resolved reflective spectrum , the result indicates the anti-reflective characteristic of cells with QDs is better than reference cell over a broadband wavelength range. We prove that the cell with QDs has the anti-reflectance coating effect.

From the J-V curve, the GaN solar cell with QDs layer can effectively enhance the short-circuit current density from 0.95 to 1.01 mA/cm^2 and the power conversion efficiency from 0.97 to 1.03 %, corresponding to a 7.2 % enhancement compared to reference ones. The overall shape of EQE enhancement resembles the absorption curves of QDs, and we believe this is a strong indication of QD absorption and down-conversion process. The enhancement is higher before 400nm, just mapping to the absorption spectrum from quantum dots.

Reference

[1] “World energy outlook 2009”, International Energy Agency, 2009.

[2] 戴寶通 and 鄭晃忠, 太陽能電池技術手冊, 1 ed.: 台灣電子材料與元件協會, 1998.

[3] 林明獻, 太陽能電池技術入門, 2 ed.: 全華圖書股份有限公司, 1998.

[4] 黃惠良, et al., 太陽電池, 1 ed.: 五南圖書出版股份有限公司, 1998.

[5] M. Yamaguchi, et al., "GaAs solar cells grown on Si substrates for space use," Progress in Photovoltaics: Research and Applications, vol. 9, pp. 191-201, 2001.

[6] M. Yamaguchi, "III-V compound multi-junction solar cells: present and future," Solar energy materials and solar cells, vol. 75, pp. 261-269, 2003.

[7] O. Jani, H. Yu, E. Trybus, B. Jampana, I. Ferguson, A. Doolittle, C. Honsberg, “Effect of phase separation on performance of III-V nitride solar cells,” in 22nd European Photovoltaic Solar Energy Conference, Milan, Italy, Sep. 3-7, 2007.

[8] X.-M. Cai, S.-W. Zeng, and B.-P. Zhang, “Fabrication and characterization of InGaN p-i-n homojunction solar cell,” Appl. Phys. Lett., vol. 95, no. 17, pp. 173504-3, Oct. 2009.

[9] C. Boney, I. Hernandez, R. Pillai, D. Starikov, A. Bensaoula, M. Henini, M. Syperek, J. Misiewicz, and R. Kudrawiec, “Growth and characterization of InGaN for photovoltaic devices,” Phys. Stat. Sol. (c), vol. 8, no. 7-8, pp. 2466-2668, Jul. 2011.

[10] P. M. F. J. Costa, R. Datta, M. J. Kappers, M. E. Vickers, C. J. Humphreys, D. M. Graham, P. Dawson, M. J. Godfrey, E. J. Thrush, J. T. Mullins, “Misfit dislocations in In-rich InGaN/GaN quantum well structures,” Phys. Stat. Sol. (a), vol. 203, no. 7, pp. 1729-1732, May 2006.

[11] David Holec, Yucheng Zhang, D. V. Sridhara Rao, Menno J. Kappers, Clifford McAleese, and Colin J. Humphreys, “Equilibrium critical thickness for misfit

dislocations in III-nitrides," J. Appl. Phys., vol. 104, no. 12, pp. 123514-7, Dec. 2008.

[12] C. J. Neufeld, N. G. Toledo, S. C. Cruz, M. Iza, S. P. DenBaars, and U. K. Mishra, Appl. Phys. Lett. 93, 143502 (2008).

[13] J. Shim. S. Jeon, Y. Jeong, and D. Lee, IEEE Electron Device Lett. 31, 1140 (2010).

[14] D. Cherns, S. Henley, and F. Ponce, Appl. Phys. Lett. 78, 2691 (2001).

[15] J. Wierer, A. Fischer, and D. Koleske, Appl. Phys. Lett. 96, 051107 (2010).

[16] K.W. J. Barnham and G. Duggan, "A new approach to high-efficiency multi-band-gap solar cells," J. Appl. Phys., vol., 67, no. 7, pp. 3490-3493, Apr. 1990.

[17] O. Jani, I. Ferguson, C. Honsberg, and S. Kurtz, Appl. Phys. Lett. 91, 132117 _2007_.

[18] J. Wu, W. Walukiewich, K. M. Yu, W. Shan, J. W. Ager, E. E. Haller, H. Lu, W. J. Schaff, W. K. Metzger, and S. Kurtz, J. Appl. Phys. 94, 6477 _2003_.

[19] Y. Nanishi, Y. Satio, and T. Yamaguchi, Jpn. J. Appl. Phys., Part 1 42, 2549 _2003_.

[20] M. Vazquez, C. Algora, I. Rey-Stolle, and J. R. Gonzalez, Progr. Photovoltaics 15, 477 (2007).

[21] C. J. Neufeld, N. G. Toledo, S. C. Cruz, M. Iza, S. P. DenBaars, and U. K. Mishra, Appl. Phys. Lett. 93, 143502 _2008_.

[22] A. De Vos, Endoreversible Thermodynamics of Solar Energy Conversion_Oxford University Press, Oxford, 1992, p. 90.

[23] I. Ho and G. B. Stringfellow, Appl. Phys. Lett. 69, 2701 _1996_.

[24] S. Y. Karpov, 3, 16 (1998).

[25] Jeffery L. Gray, "The Physics of the Solar Cell," in Handbook of Photovoltaic Science and Engineering, John Wiley & Sons, New York, 61-111, (2003).

[26] Sze S, Physics of semiconductor Devices, 3rd Edition, John Wiley & Sons, New York, 719-741, (2007).

[27] S. Sze and K. Ng, Physics of semiconductor devices: Wiley-Blackwell, 2007.

[28] D. Neamen, Semiconductor physics and devices: McGraw-Hill, Inc. New York, NY,

USA, 2002.

[29] 莊家琛,“太陽能工程-太陽能電池篇,” 全華出版社 (2005).

[30] M. P. Thekackra, “The Solar Cell Constant and Solar Spectrum Measurement from a Research Aircraft,” NASA Technical Report, (1970).

[31] D. A. Neamen, “Semiconductor Physics and Devices,” (2003).

[32] http://en.wikipedia.org/wiki/Scanning_electron_microscope

[33] http://en.wikipedia.org/wiki/PECVD

[34] D. Neamen, Semiconductor physics and devices: McGraw-Hill, Inc. New York, NY, USA, 2002.

[35] K. Sato, M. Shikida, T. Yamashiro, M. Tsunekawa, and S. Ito, Sensors and Actuators a-Physical **73** (1-2), 122 (1999).

[36] E. D. Palik, O. J. Glembocki, I. Heard, P. S. Burno, and L. Tenerz, Journal of Applied Physics **70** (6), 3291 (1991).

[37] M. M. Caldwell, “Plant life and ultraviolet radiation: some perspective in the history of the earth's UV climate,” Bioscience 29(9), 520–525 (1979).

[38] Q. Sun, Y. A. Wang, L. S. Li, D. Wang, T. Zhu, J. Xu, C. Yang, and Y. Li, “Bright, multicoloured light-emitting diodes based on quantum dots,” Nat. Photonics 1(12), 717–722 (2007).

[39] T. Trupke, M. A. Green, and P. Würfel, “Improving solar cell efficiencies by down-conversion of high-energy photons,” J. Appl. Phys. 92(3), 1668–1674 (2002).

[40] E. Matioli et al., Appl. Phys. Lett. 98, 021102 (2011).

[41] H.C. Chen et al., 12 March 2012 / Vol. 20, No. S2 / OPTICS EXPRESS